GBSとガングリオシド複合体抗体－最近の知見

近畿大学医学部神経内科教授　楠　　進

key words　Guillain-Barré syndrome, Fisher syndrome, autoimmune neuropathy, ganglioside, ganglioside complex

要　旨

末梢神経の自己免疫疾患であるGuillain-Barré症候群（GBS）では，抗ガングリオシド抗体が高頻度に上昇し，診断マーカーおよび発症因子として注目されている．近年二つのガングリオシドの糖鎖の相互作用で生ずるエピトープであるガングリオシド複合体に対する抗体が見出された．最初に報告されたGD1a/GD1b複合体に対する抗体は，人工呼吸器使用の必要な重症例に高頻度にみられる．GM1/GalNAc-GD1a複合体抗体は純粋運動型GBSにみられ，運動神経幹中間部に病初期から伝導ブロックが見られるのが特徴である．またFisher症候群ではGQ1b抗体が90%以上にみられるが，GQ1bとGM1あるいはGD1aなどの複合体により強く反応する抗体があることもわかった．神経障害の機序として，抗体の結合に続く補体やマクロファージによる細胞膜の傷害の他に，ラフトへの結合を介した細胞機能障害やアポトーシスの可能性も考えられ，今後の詳細な検討が必要である．

動　向

Guillain-Barré症候群（GBS）は末梢神経を標的とする自己免疫疾患であり，自己抗体を中心とする液性免疫と細胞性免疫の両面から数多くの解析が行われてきた．とくに治療として血漿交換が有効であることから，自己抗体をはじめとする液性因子の病態への関与が重要と考えられた．その中で，特異性と陽性率の高いものとして，ガングリオシドの糖鎖を認識する抗ガングリオシド抗体が見出され注目されている．ガングリオシドは糖鎖構造にもとづいて多くの分子種があり，抗体の反応するガングリオシドの種類も症例ごとにさまざまである[1-3]．

高い抗体価のIgGタイプの抗ガングリオシド抗体は，GBSおよび関連疾患の患者血中にしばしばみられるが，他の自己免疫疾患や神経疾患では通常みられない．したがってIgG抗ガングリオシド抗体の上昇は，GBSに特徴的なことである．発症直後の検体で抗体価がピークとなり，経過とともに低下・消失するという経過から，抗体の上昇は神経障害の結果ではなく病態と密接に関連するものと考えられる．GBSにおける抗ガングリオシド抗体産生のメカニズムとしては，先行感染の病原因子がガングリオシド類似の糖鎖構造をもつという「分子相同性機序」が提唱されている．

GBSではさまざまな抗ガングリオシド抗体がみられ，それぞれの抗体は特有の臨床病型と対応

している．その対応は標的抗原の局在により説明できる例が多い[2,3]．したがって抗体は，標的となるガングリオシドに結合することで，そのガングリオシドが分布する部位を特異的に障害するという可能性が考えられる．その対応が最も明確なのが，GBSの亜型であるFisher症候群（FS）の急性期血清で90%以上の高頻度にみられる抗GQ1b IgG抗体であり，眼球運動を支配する脳神経である動眼神経・滑車神経・外転神経のRanvier絞輪部周囲（傍絞輪部）ミエリンに高濃度に局在するGQ1bに結合して眼球運動麻痺をきたすことが示唆されている[4]．

ガングリオシドは神経組織に多く含まれ，細胞膜の構成成分であり糖鎖を細胞外に向ける形で存在している．上記のように多くの分子種があり，それぞれが神経組織内で独特の分布を示す．近年，ガングリオシドなどのスフィンゴ脂質は，リン脂質の膜の中に集簇して存在しラフト（いかだ）を形成すると考えられている．こうした構造はリピドラフトあるいは脂質マイクロドメインと呼ばれ，そこにはシグナル伝達，突起伸展，シナプス形成，接着などの神経細胞にとって重要な過程に関与するさまざまなタンパク分子が局在することが明らかになってきている[5,6]．

A. GBSにおけるガングリオシド複合体に対する抗体

最近我々は2種類のガングリオシドを混合し作製した複合抗原に対する抗体をGBSの急性期血清に見出した[7]．これは単独のガングリオシド抗原にはほとんど反応しないが，2種のガングリオシドを混合した抗原に強く反応するものである．この抗体は二つの抗原が形成する新たな複合エピトープを特異的に認識していると考えられる．我々はこの複合抗原をガングリオシド複合体ganglioside complex（GSC）と名付け，GBSおよびその亜型において抗GSC抗体の意義を調べている．

1. GD1a/GD1b複合体抗体

ガングリオシド複合体に対する抗体として最初に見出されたのは，GD1aとGD1bの複合体（GD1a/GD1b）に対する抗体である[7]．ある重症のGBS患者血清IgGが，ルーチンで行っている11種類の抗原に対していずれも反応を示さず，未精製のウシ脳ガングリオシドに薄層クロマトグラム免疫染色で強い反応を示した．当初は未同定の微量ガングリオシドに対する抗体と考え，その抗原をカラム操作により精製することを試みた．従来GalNAc-GD1aやGM1bをGBSの標的抗原として見出したときと同様に考えたわけである．しかし，何度か試みたがそのたびに，精製前には非常に強かった反応は精製の最終段階に入ると弱いものになっていった．ある時，その抗原の移動度がGD1aとGD1bに近いものであったことから，その2つからなる抗原を認識しているのではないかと考えるに至った．そこでELISA法にて両者をひとつのウェルに入れて反応させると非常に強い反応を示した（図1）．この反応は，薄層クロマトグラム上の免疫染色にても確認され，GD1a，GD1b単独をそれぞれ別のレーンに展開して血清IgGを反応させても反応はみられないが，両者を同じレーンに展開するとGD1aの下端とGD1bの上端のオーバーラップした部分にのみ強い反応が認められた．異なる展開溶媒を用いて，GD1aとGD1bを完全に分離する条件で薄層クロマトグラムを行うと，反応はみられなくなった．したがってこの抗体はGD1aとGD1bの両者により形成されるエピトープを認識すると考えられた．その後，他のGBS血清でも同様の反応（GD1aとGD1b単独には反応しないかきわめて弱い反応しか示さないが両者の複合体に強く反応する）を示すものがあり，重症例が多い傾向がみられた．

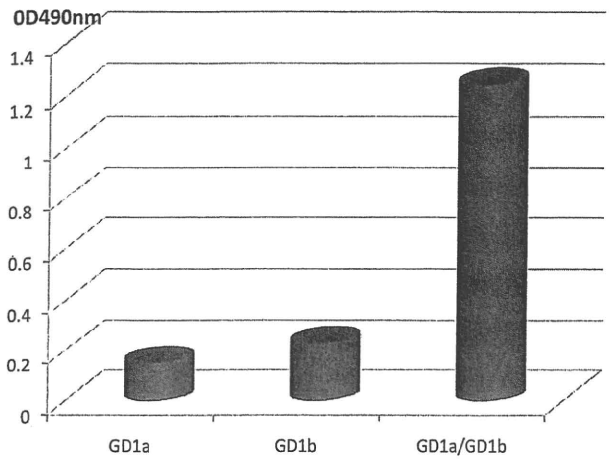

図1　ELISA法で測定したGD1a/GD1b複合体に対するIgG抗体
GD1aとGD1b単独に対しては反応がきわめて弱いが，GD1aとGD1bの混合抗原（GD1a/GD1b）に対しては強い反応を示す（文献7のPatient 1のデータを用いて作成）．

さらにGD1a/GD1b以外の複合体，すなわちGM1/GD1a，GD1b/GT1b，GM1/GT1bなどに対する抗体も認められることがわかった．

そこで多数例（234例）のGBS血清について，抗原としてGM1，GD1a，GD1b，GT1bを用い，そのうちの2つの組み合わせの混合抗原（6種類）に対する抗体活性をみたところ，39例（17%）にいずれかの複合体に対する抗体がみられた．そのうち，GD1a/GD1b（およびGD1b/GT1b）に対する抗体は，呼吸筋麻痺をきたす重症GBSにみられる頻度が有意に高いことがわかった[8]．抗GD1a/GD1b複合体抗体のELISA法の結果を図1に示す．

2. GM1/GalNAc-GD1a複合体抗体

GM1およびGalNAc-GD1aはいずれも軸索障害型のGBSにおける血中抗体の標的抗原として知られる．GM1とGalNAc-GD1aの混合抗原に対するGBS急性期血中抗体を検討したところ，GM1やGalNAc-GD1aそれぞれについては抗体活性がみられないかきわめて低いが，両者の混合抗原に強い反応がみられ，GM1/GalNAcGD1a複合体抗体陽性と判断される例が数%あることがわかった[9]．抗GM1/GalNAc-GD1a抗体陽性GBS10例の検討では，ほとんどが純粋運動型GBSであり，生理的圧迫部位ではなく運動神経幹中間部に，病初期から伝導ブロックが10例中5例に見られた．Haddenらの判定基準[10]では，10例中4例が脱髄型で2例が軸索型，Hoらの基準[11]では4例が脱髄型で3例が軸索型であった．ただ，この抗体陽性例の伝導ブロックは治療後早期に回復し，経過を通じて再髄鞘化を示す所見に乏しいことからRanvier絞輪部における軸索機能障害による可逆性伝導障害の可能性が考えられる．運動神経Ranvier絞輪部軸索膜に集簇して存在するGM1，GalNAc-GD1aが複合体を形成し純粋運動型GBSの標的抗原となっている可能性がある．

CapassoらはGBSのひとつの型としてacute motor conduction block neuropathy（AMCBN）という概念を提唱し[12]，GM1などのガングリオシド抗体との関連も述べているが，GM1抗体陽性の多くは軸索障害型でAMCBNの病型を示す例は少数である．したがってGM1/GalNac-GD1a抗体はAMCBNの病型により強く関連する抗体と考えられる．

3. GQ1bを構成要素に含む複合体に対する抗体

FSでは前述のようにGQ1bに対する抗体が90%以上の頻度でみられる．そしてGQ1bと同じ糖鎖末端をもつGT1aにも交差反応を示すことが多い．しかし，GBSにおけるガングリオシド複合体抗体の存在を考え，GQ1bあるいはGT1aに他のガングリオシドを混合した抗原と血清との反応を検討したところ，GQ1bあるいはGT1aを含むGSCに対する反応がGQ1bやGT1aそのも

のよりも強い（すなわちGSCに対して特異性をもつ）抗体が約半数に認められることがわかった[13]．そして多数例の検討からFSや眼球運動麻痺を伴うGBSにおける抗ガングリオシド抗体は反応特異性の点から，(1) GQ1bやGT1aに特異的な抗体，(2) GQ1b/GM1あるいはそれと同様に末端糖鎖がジシアロシル基とGal-GalNAc基の組み合わせとなるGSC（GQ1b/GM1, GQ1b/GD1b, GT1a/GM1, GT1a/GD1b）特異的抗体，(3) GQ1b/GD1aあるいはそれと同様に末端糖鎖がジシアロシル基とシアロシルGal-GalNAc基の組み合わせとなるGSC（GQ1b/GD1a, GT1a/GD1a, GQ1b/GT1b, GT1a/GT1b）特異的抗体の3つに分類されることが明らかとなった（図2）[14]．またGQ1b/GA1を認識する抗体も報告されている[15]．

FSではGQ1bが重要な標的抗原であることは間違いないが，症例によっては血中抗体が細胞膜上でGQ1bとGM1あるいはGD1aが形成したGSCをより強く認識する場合があるわけである．臨床症状をみると，抗GQ1b/GM1抗体陽性例では感覚障害の少ない傾向が見られるが[13,14]，抗体の反応性の違いがどのような臨床的意義をもつかは今後の検討が必要である．

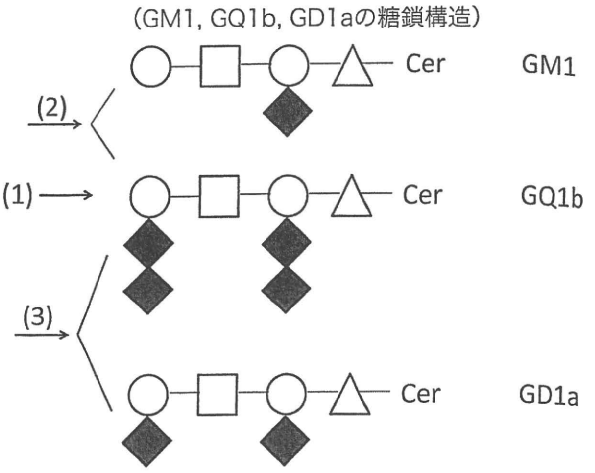

図2　Fisher症候群（FS）の血中抗体の反応特異性
FSの血中抗体は (1) GQ1bに特異的に反応する抗体，(2) GQ1bとGM1の形成する複合体により強く反応する抗体，(3) GQ1bとGD1aの形成する複合体により強く反応する抗体，の3種類に大別される．
○: ガラクトース，□: N-アセチルガラクトサミン，△: グルコース，◆: シアル酸，Cer: セラミド

B. ガングリオシド複合体抗体の産生機序

GBSおよび関連疾患におけるガングリオシド抗体の産生機序としては，先行感染の病原因子のもつ糖鎖がガングリオシドに類似しており，先行感染因子に対する免疫反応の結果抗ガングリオシド抗体が産生されるという「分子相同性機序」が提唱されている．Kuijfらは，GM1/GD1a抗体やGQ1b/GD1a抗体が，先行感染の原因となった*Campylobacter jejuni*のリポオリゴ糖と交差反応したことを報告した[16]．このことは，GSCに対する抗体もガングリオシド抗体と同様の機序で産生されることを示唆しているが，直接的な証明は今後の課題である．

C. 他のニューロパチーにおけるガングリオシド複合体抗体

Nobile-Orazioらは，慢性炎症性脱髄性多発ニューロパチー（CIDP），多巣性運動ニューロパチー，IgMパラプロテイン血症を伴うニューロパチー（PN-IgM），などの慢性ニューロパチーにおけるガングリオシド複合体に対する抗体を検討した．その結果，34例のCIDP中1例においてGT1b/GM1およびGT1b/GM2に対するIgM抗体を，23例のPN-IgM中1例にGM2/GD1bに対するIgM抗体をそれぞれ検出したと報告している[17]．陽性率は低いが，GBS以外の免疫性ニューロパチーにおいてもガングリオシド複合体が標的となり得ることが示されたわけである．

D. 単独のガングリオシドに特異的な抗体と複合体の反応

異なる2つのガングリオシドが相互作用で新たなエピトープを作っていることは，あるガングリオシド特異的抗体の反応が当該ガングリオシドと他のガングリオシドが形成したGSCに対して弱くなることから支持される．

ルーチンの抗体測定でGD1bに対するIgG抗体のみがみられたGBS血清について，GD1bに他のガングリオシドを加えた混合抗原に対する反応をみたところ，GM1を加えても反応の強さは変わらなかったが，GD1a, GT1a, GalNAc-GD1aなどを加えると反応が著明に減弱した[18]．したがってGD1bの糖鎖はそれらのガングリオシドの糖鎖と相互作用してコンフォメーションを変化させやすいと考えられる．

GD1b抗体は従来から運動失調との関連が報告されているが[19]，同抗体陽性例全例が運動失調を伴うわけではなく，その理由は不明であった．前記のGD1b抗体の反応性の減弱の程度を，運動失調を伴う例と伴わない例で比較したところ，伴う例では有意に減弱の程度が強かった[18]．運動失調を伴うGBSでみられるGD1b抗体は，GD1bに対する特異性がきわめて高く，GD1bのわずかな三次元的コンフォメーションの変化によって反応できなくなったと考えられ，この特異性の違いが運動失調を伴うか伴わないかに関連することが示唆された．

単独のガングリオシドに対する抗体の反応が，他のガングリオシドが共存することにより減弱することは，上記のGQ1b抗体についてもみられており[14]，またGM1抗体について他のグループからも報告されている[20]．

E. 今後の検討課題

GSCに対する反応性の検証を行うことにより，ガングリオシド抗体の診断マーカーとしての有用性は向上する．GBSでこれまでに報告された代表的なGSCs抗体を表1に示す．GSC抗体の発見以来，我々の研究室では重症例と関連するGD1a/GD1b抗体をGBSではルーチンに測定し，その他のGSCに対する抗体も適宜測定している．今後さらに新たなGSCが見出される可能性がある．それらを含めて，GSCの神経系における局

表1　GBSおよび関連疾患における代表的ガングリオシド複合体抗体

抗原	疾患	頻度（%）	臨床病型
GD1a/GD1b	GBS	7	重症GBS
GD1b/GT1b	GBS	6	重症GBS
GM1/GalNAc-GD1a	GBS	4	純粋運動型GBS AMCBN
GQ1b/GM1および	FS	41	感覚障害が少ない
関連するGSCs	GBS with OP	28	
GQ1b/GD1aおよび	FS	6	
関連するGSCs	GBS with OP	19	

GSC: ganglioside complex, GBS: Guillain-Barré syndrome, FS: Fisher syndrome
AMCBN: acute motor conduction block neuropathy
OP: ophthalmoplegia
GQ1b/GM1および関連するGSCs: GQ1b/GM1, GQ1b/GD1b, GT1a/GM1, GT1a/GD1b
GQ1b/GD1aおよび関連するGSCs: GQ1b/GD1a, GT1a/GD1a, GQ1b/GT1b, GT1a/GT1b

在の解明やGSCs抗体による神経障害の動物モデル作成も必要であろう.

また最近の研究でGSCは単独ガングリオシドよりも細胞内情報伝達に強い影響を及ぼす可能性が指摘されている[21]. したがってGSC抗体による神経障害については, 補体活性化を介する傷害だけではなく, 神経細胞機能の直接的障害やアポトーシス[22]などのメカニズムも今後検討する必要があろう.

文献

1) Van Doorn P, Ruts L, Jacobs B. Clinical features, pathogenesis, and treatment of Guillain-Barré syndrome. Lancet Neurol. 2008; 7: 939-50.
2) Kusunoki S, Kaida K, Ueda M. Antibodies against gangliosides and ganglioside complexes in Guillain-Barré syndrome: New aspects of research. Biochim Biophys Acta. 2008; 1780: 441-4.
3) Kaida K, Kusunoki S. Antibodies to gangliosides and ganglioside complexes in Guillain-Barré syndrome and Fisher syndrome: mini-review. J Neuroimmunol. 2010; 223: 5-12.
4) Chiba A, Kusunoki S, Obata H, et al. Serum anti-GQ1b IgG antibody is associated with ophthalmoplegia in Miller Fisher syndrome and Guillain-Barré syndrome: Clinical and immunohistochemical studies. Neurology. 1993; 43: 1911-7.
5) Hakomori S. The glycosynapse. Proc Natl Acad Sci U S A. 2002; 99: 225-32.
6) Simons K, Ikonen E. Functional rafts in cell membranes. Nature. 1997; 387: 569-72.
7) Kaida K, Morita D, Kanzaki M, et al. Ganglioside complexes as new target antigens in Guillain-Barré syndrome. Ann Neurol. 2004; 56: 567-71.
8) Kaida K, Morita D, Kanzaki M, et al. Anti-ganglioside complex antibodies associated with severe disability in GBS. J Neuroimmunol. 2007; 182: 212-8.
9) Kaida K, Sonoo M, Ogawa G, et al. GM1/GalNAc-GD1a complex: A target for pure motor Guillain-Barré syndrome. Neurology. 2008; 71: 1683-90.
10) Hadden RDM, Cornblath DR, Hughes RA, et al. Electrophysiological classification of Guillain-Barré syndrome: clinical associations and outcome: Plasma Exchange/Sandoglobulin Guillain-Barré Syndrome Trial Group. Ann Neurol. 1998; 44: 780-8.
11) Ho TW, Mishu B, Li CY, et al. Guillain-Barré syndrome in northern China. Relationship to Campylobacter jejuni infection and anti-glycolipid antibodies. Brain. 1995; 118: 597-605.
12) Capasso M, Caporale CM, Pomilio F, et al. Acute motor conduction block neuropathy: another Guillain-Barré syndrome variant. Neurology. 2003; 61: 617-22.
13) Kaida K, Kanzaki M, Morita D, et al. Anti-ganglioside complex antibodies in Miller Fisher syndrome. J Neurol Neurosurg Psychiatry. 2006; 77: 1043-6.
14) Kanzaki M, Kaida K, Ueda M, et al. Ganglioside complexes containing GQ1b as targets in Miller Fisher and Guillain-Barré syndrome. J Neurol Neurosurg Psychiatry. 2008; 79: 1148-52.
15) Ogawa G, Kaida K, Kusunoki S, et al. Antibodies to ganglioside complexes consisting of asialo-GM1 and GQ1b or GT1a in Fisher and Guillain-Barré syndromes. J Neuroimmunol. 2009; 214: 125-7.
16) Kuijf, ML, Godschalk, PC, Gilbert, M, et al. Origin of ganglioside complex antibodies in Guillain-Barré syndrome. J Neuroimmunol. 2007; 188: 69-73.
17) Nobile-Orazio E, Giannotta C, Briani C. Anti-ganglioside complex IgM antibodies in multifocal motor neuropathy and chronic immune-mediated neuropathies. J Neuroimmunol. 2009; 219: 119-22.
18) Kaida, K, Kamakura, K, Ogawa, G, et al. GD1b-specific antibody induces ataxia in Guillain-Barré syndrome. Neurology. 2008; 71: 196-201.
19) Kusunoki S, Shimizu J, Chiba A, et al. Experimental sensory neuropathy induced by sensitization with ganglioside GD1b. Ann Neurol. 1996; 39: 424-31.
20) Greenshields KN, Halstead SK, Zitman FM, et al. The neuropathic potential of anti-GM1 autoantibodies is required by the local glycolipid environment in mice. J Clin Invest. 2009; 119:

595-610.
21) Todeschini AR, Dos Santos JN, Handa K, et al. Ganglioside GM2/GM3 complex affixed on silica nanospheres strongly inhibits cell motility through CD82/cMet-mediated pathway. Proc Natl Acad Sci U S A. 2008; 105; 1925-30.
22) Takada K, Shimizu J, Kusunoki S. Apoptosis of primary sensory neurons in GD1b-induced sensory ataxic neuropathy. Exp Neurol. 2008; 209: 279-83.

Journal of Cellular Physiology

Establishment of a New Conditionally Immortalized Human Brain Microvascular Endothelial Cell Line Retaining an In Vivo Blood–Brain Barrier Function

YASUTERU SANO,[1] FUMITAKA SHIMIZU,[1] MASAAKI ABE,[1] TOSHIHIKO MAEDA,[1] YOKO KASHIWAMURA,[1] SUMIO OHTSUKI,[2] TETSUYA TERASAKI,[2] MASUO OBINATA,[3] KOJI KAJIWARA,[4] MASAMI FUJII,[4] MICHIYASU SUZUKI,[4] AND TAKASHI KANDA[1]*

[1]*Department of Neurology and Clinical Neuroscience, Yamaguchi University Graduate School of Medicine, Ube, Yamaguchi, Japan*

[2]*Department of Molecular Biopharmacy and Genetics, Graduate School of Pharmaceutical Sciences, Tohoku University, Sendai, Miyagi, Japan*

[3]*Department of Cell Biology, Institute of Development, Aging and Cancer, Tohoku University, Sendai, Miyagi, Japan*

[4]*Department of Neurosurgery, Yamaguchi University Graduate School of Medicine, Ube, Yamaguchi, Japan*

The breakdown of the blood–brain barrier (BBB) has been considered to be a key step in the disease process of a number of neurological disorders such as cerebral ischemia and Alzheimer's disease. Many in vitro BBB models derived from animal tissues have been established to elucidate the mechanism of BBB insufficiency. However, only a few human immortalized in vitro BBB models have been reported. In the present study, a temperature-sensitive SV40-T antigen was introduced to immortalize cells using a retrovirus to obtain a better human in vitro BBB model which sustains physiological properties. This endothelial cell (EC) line, termed TY08, showed a spindle-shaped morphology. The cells expressed all key tight junctional proteins, such as occludin, claudin-5, zonula occludens (ZO)-1 and ZO-2 at their cell-to-cell boundaries, and had low permeability to inulin across its monolayer. The cells also expressed various influx and efflux transporters and exhibited the functional expression of *p*-glycoprotein. Furthermore, the TY08 cells grew and proliferated well under the permissive temperature and stopped growing under the non-permissive temperature to serve as physiological ECs forming the BBB. Thus, conditionally immortalized TY08 cells retaining the in vivo BBB functions should facilitate analyses for determining the pathophysiology of various neurological diseases.

J. Cell. Physiol. 225: 519–528, 2010.

The blood–brain barrier (BBB) is formed from a continuous monolayer of highly specialized endothelial cells (ECs). The features that distinguish brain microvascular endothelial cells (BMECs) from those of peripheral organs include their formation of impermeable intercellular tight junctions (TJs), a paucity of pinocytotic vesicles, the expression of specific transporters, and expression of enzymes such as γ-glutamyl transpeptidase and alkaline phosphatase (Joó, 1996). Cultured BMECs are an important in vitro BBB model that can be used to analyze the physiological and biological functions of the BBB, as well as to estimate the BBB permeability of compounds. To date, many cell culture systems have been established as in vitro BBB models (Terasaki et al., 2003). Most of these cultured cells have been derived from animals such as cows, pigs, mice, and rats because their use is practical and economical. In contrast, the models derived from the human brain, especially those involving extensively characterized cells (Weksler et al., 2005) are rare. However, an in vitro BBB model derived from the human brain would be useful for analyzing the function of the BBB under both physiological and pathological conditions, since species differences may exist. Generally, primary cultured human BMECs (HBMECs) rapidly undergo senescence even upon limited passages. Therefore, most of the in vitro BBB models established so far were immortalized using a tumor gene such as simian virus 40 (SV40) large T-antigen (Muruganandam et al., 1997) or the E6 and E7 genes of the human papilloma virus (Kusch-Poddar et al., 2005; Ketabi-Kiyanvash et al., 2007). However, immortalized cells often act like tumor cells and lose the morphological and physiological properties of the parental cells. Recently, conditionally immortalized BMECs were established by using a transgenic rat harboring a temperature-sensitive SV40 large T-antigen gene (Hosoya et al., 2000). These cells show better maintenance of their in vivo function as BBB-constituting endothelium (Hosoya et al., 2000; Terasaki et al., 2003). The gene product of the temperature-sensitive SV40 large T-antigen (tsA58) is in an

Contract grant sponsor: Japan Society for the Promotion of Science, Tokyo, Japan;
Contract grant numbers: 18390259, 19790610.

*Correspondence to: Takashi Kanda, Department of Neurology and Clinical Neuroscience, Yamaguchi University Graduate School of Medicine, 1-1-1 Minami-kogushi, Ube, Yamaguchi 755-8505, Japan. E-mail: tkanda@yamaguchi-u.ac.jp

Received 17 May 2009; Accepted 21 April 2010

Published online in Wiley Online Library (wileyonlinelibrary.com.), 10 May 2010.
DOI: 10.1002/jcp.22232

active conformation and binds to p53 at 33°C, thus facilitating the immortalization of the cells, whereas the conformation of the gene product changes leading to its degradation and the release of p53 when the cells are grown at 37°C (Jat and Sharp, 1989). The tsA58 protein is inactivated by shifting the culture temperature to 37°C, and under that condition, cell growth is repressed or arrested, and the cells again resemble the parental, non-immortalized cells. Therefore, these cell lines are conditionally immortal. We used this concept to establish a new human in vitro BBB model. Herein, we present out data demonstrating that a new in vitro human BBB model harboring the tsA58 protein was successfully generated using a retrovirus. The BBB-specific properties of the cell lines were extensively characterized, and our results indicate that this new in vitro human BBB model retains the salient features of the BBB, and can therefore be useful for estimating the drug permeability across the human BBB and to understand the mechanism of BBB insufficiency in a number of neurological diseases.

Materials and Methods

Materials

Polyclonal rabbit anti-occludin, rabbit anti-zonula occludens-1 (ZO-1), and rabbit anti-claudin-5 antibodies were obtained from Zymed (San Francisco, CA). FITC-conjugated secondary antibodies were also purchased from Zymed. A monoclonal anti-*p*-glycoprotein (*p*-gp) antibody was obtained from Signet Laboratories (Dedham, MA). Polyclonal goat anti-ZO-2, anti-von Willebrand factor (vWF) antigen, and monoclonal anti-actin antibodies were obtained from Santa Cruz Biotechnologies (Santa Cruz, CA). The polyclonal anti-SV40 T antigen antibody was purchased from Calbiochem (Darmstadt, Germany). Calcein-acetoxymethylester (calcein-AM) was obtained from Molecular probes (Eugene, OR). Verapamil was purchased from WAKO (Osaka, Japan). Rhodamine 123 and novobiocin were obtained from Sigma (St. Louis, MO). MK-571 was obtained from Biomol (Plymouth Meeting, PA). The retrovirus vector pDON-AI was purchased from TAKARA Bio Inc. (Ostu, Japan).

Culture media

The dissecting medium (DM) contained Dulbecco's modified Eagle's medium (DMEM; Sigma) supplemented with 5% fetal bovine serum (FBS; Sigma), 100 U/ml penicillin (Sigma), 100 μl/ml streptomycin (Sigma), and 25 ng/ml amphotericin B (Invitrogen, Grand Island, NY). EC growth medium contained EBM-2 medium (Cambrex, Walkersville, MD) supplemented with 20% FBS, EGM-2 MV (Cambrex), 100 U/ml penicillin (Sigma), 100 μl/ml streptomycin (Sigma), and 25 ng/ml amphotericin B (Invitrogen).

Isolation of human brain microvascular endothelial cells

The study protocol for human brain tissue was approved by the ethics committee of the Medical Faculty of Yamaguchi University, and was conducted in accordance with the Declaration of Helsinki, as amended in Somerset West in 1996. Written informed consent was obtained from the participant before entering the study. Tissue samples were obtained from the normal brain tissue of a patient with a large meningioma located in left medial middle fossa. Meningiomas originate from the meninges, and the surrounding brain tissue is normal if there is no invasion. No invasion into the brain was observed in our patient in either the macroscopic or microscopic findings. The tumor was covered with normal brain tissue, and it was necessary to remove the tip of the normal left temporal lobe to safely remove the entire tumor. This procedure is relatively common, and patients usually do not experience any significant postoperative symptoms after the removal of this part of the brain. Informed consent was obtained from the patient before the operation to remove this portion of the normal brain and to use the tissue for this study. HBMECs were isolated in accordance with a previously described procedure (Kanda et al., 1994) with modifications. Briefly, brain tissue was freed of meninges and surface vessels with fine forceps, dissected into 5 mm pieces and then was homogenized in a Potter–Elvehjem homogenizer. The homogenate was digested with 0.005% dispase (Sigma) in DM at 37°C for 2 h in a shaking water bath. After centrifugation (800*g*, 5 min), the pellet was suspended with DM. The sample was added to the same volume of 32% dextran, resulting in a 16% dextran solution (mol wt 70,000; 16% wt/vol in DM; Sigma) and the whole suspension was centrifuged (4,500*g*, 15 min, 4°C). The pellet was re-suspended with the dextran solution and centrifuged again. The resulting pellet was recovered with DM and filtered through a 190-μm nylon filter mesh (Tetko Inc., Briarcliff Manor, NY) to remove large vessels. The filtrate was collected and further digested with 0.025% collagenase/dispase (Sigma) in 1 × Hanks' balanced salt solution (HBSS; Invitrogen) at 37°C for 6 h in a shaking water bath. After centrifugation (800*g*, 5 min), the pellet was washed with DM twice and recovered with 1.0 ml DM. The pellets were passed through a filter with a 15-μm pore (Tetko Inc.), and the trapped cells were placed on a type I collagen-coated dish (Iwaki, Tokyo, Japan). The cells were cultured at 37°C in a humidified atmosphere of 5% CO_2 and 95% air.

Immortalization and purification of HBMECs

Seven days after the first dissemination, the cells were incubated overnight with pDON-AI/tsA58, a retroviral vector encoding the open reading frame of the temperature-sensitive SV40 large T-antigen. After 24 h, the cells were washed with HBSS several times and were subsequently grown at 33°C. When ECs grew sufficiently for cloning, they were picked up with a cloning cup. Non-ECs such as pericytes, astrocytes, and fibroblasts also appeared as the ECs grew and gradually began to occupy the culture area of the dish. These non-ECs were scratched and removed mechanically with a sterilized pointed rubber scraper. One clonal population consisting of pure ECs, designated "TY08" was obtained after three passages for cloning. These TY08 cells showed robust proliferation at a permissive temperature of 33°C. These cells were then fully characterized.

Identification of HBMECs

HBMECs were identified based on the following three criteria: spindle-shaped morphology; immunoreactivity to an anti-vWF antigen antibody, and uptake of 1,1'-dioctacecyl-3,3,3',3', tetramethyl indocarbocyanine perchlorate acetylated low-density lipoprotein (DiI-Ac-LDL; Biogenesis, Poole, England). To label them with DiI-Ac-LDL, the cells were incubated with 10 μg/ml DiI-Ac-LDL at 33°C in the culture medium overnight. Cells were subsequently viewed under a fluorescence microscope (Olympus, Tokyo, Japan). HBMECs incorporated bright DiI-Ac-LDL particles into their cytoplasm.

Cell growth study

To determine the doubling time of the TY08 cells, 5.0×10^4 cells were seeded on type I collagen-coated 35-mm dishes and grown at 33 and 37°C. After a predetermined period, the cells were trypsinized and counted using a hemocytometer.

Immunocytochemistry

Cells (1×10^6) were seeded on rat tail collagen type I-coated 35-mm dishes (BD Bioscience, Franklin Lakes, NJ) at 33°C and grown to confluence. The confluent cells were then washed three times with PBS. The cells were fixed in 4% paraformaldehyde (Wako) for 15 min at room temperature in preparation for vWF immunocytochemistry. Next, the cells were permeabilized with 0.1% Triton X-100 (Sigma) for 10 min and then blocked with 1% BSA in PBS for 1 h. The cells were fixed with 100% ethanol for 30 min at 4°C for the staining of claudin-5, occludin, ZO-1, and ZO-2, then, were washed three times in PBS, permeabilized with

1% Triton X-100 for 20 min at room temperature, washed in PBS, and blocked with 0.1% FBS before staining. After several washes with PBS, the cells were incubated with the relevant antibodies (1:50 dilution) at 4°C overnight. The negative control cells were incubated with 2% FBS instead of the primary antibodies. The cells were subsequently washed with PBS and then incubated with FITC-conjugated secondary antibodies (1:200 dilution) for 1 h at room temperature. Fluorescence was detected using a fluorescence microscope (Olympus).

Transendothelial electrical resistance study

Transendothelial electrical resistance (TEER) reflects ion permeability across the monolayer of the ECs (Deri et al., 2005). The transwell inserts (pore size, 0.4 μm; effective growth area, 0.3 cm^2; BD Bioscience, Franklin Lakes, NJ) were coated with rat tail collagen type-I (BD Bioscience) in accordance with the manufacturer's instructions. Cells were seeded at 1.0×10^4 cells/insert on the collagen-coated culture inserts at 33°C. After allowing the cells to attach to the bottom of the insert (24–48 h) and become confluent, the TEER of cell layers was measured with a Millicell electrical resistance apparatus (Endohm-6 and EVOM, World Precision Instruments, Sarasota, FL). TR-BBB13 cells, derived from the tsA58 transgenic rat brain, which have been thought to suppress claudin-5 expression (Ohtsuki et al., 2007) and human umbilical vein endothelial cells (HUVECs; Japan Health Sciences Foundation, Osaka, Japan) were used as negative control ECs because they do not have sufficient TJs. Statistical significance was evaluated using Student's *t*-test.

Reverse transcription-polymerase chain reaction (RT-PCR) analysis

The cells were grown to confluence and washed three times with PBS. Total RNA was prepared from PBS-washed TY08 cells and the human cerebrum using an RNeasy® Plus Mini kit (Qiagen, Hilden, Germany). RT and PCR amplification were carried out with TAKARA PCR Thermal Cycler Dice (TakaRa). Single-stranded cDNA was synthesized from 250 ng of total RNA using the StrataScript® First Strand Synthesis System (Stratagene®, Cedar Greek, TX) with an oligo-dT primer and sequential PCR was performed with TaKaRa Ex Taq® (TaKaRa). Temperature cycling conditions for each primer consisted of 5 min at 94°C followed by 40 cycles for 1 min at 94°C, 1 min at 55–65°C, and 1 min at 72°C, with a final extension for 10 min at 72°C. The sequence specificity of each primer pair and its reference except claudin-12 are shown in Table 1. The primer pairs for claudin-12 were designed as follows: sense ctgtttccataggcagagcg and antisense aagcagattcttagccttcc (Accession number NM_012129; fragment size 364 bp). The PCR products were visualized by ethidium bromide staining following resolution on a 2% agarose gel. Products were compared to a 50-bp ladder (O'GeneRuler™ 50 bp DNA Ladder, Burlington, Canada) to estimate the band size. The size of each amplified product corresponded to the expected size described in the previous reports which were reviewed in the literature.

Permeability study

TY08 cells and TR-BBBs were seeded on 24-well tissue culture inserts (0.4 μm pore size, 1.0×10^4 cells/insert), and grown to confluence. The cells were incubated at 37°C for 30 min before the beginning of the experiment. Next, 1,200 μl of culture medium was added to the lower well and 500 μl of culture medium containing [carboxyl-^{14}C]-inulin (0.2 μCi/ml) was added to the upper compartment of each insert. After incubation for 15, 30, 45, and 60 min at 37°C, 20 μl samples from the upper and lower compartments were measured by scintillation counting. The clearance of inulin (C_{inu}) was calculated as follows: $C_{inu} = V_L \times CPM_L/CPM_U$, where V_L is the volume of the lower compartment in μl, CPM_L is the radioactivity of [carboxyl-^{14}C]-inulin in the lower chamber CPM/μl and CPM_U is the radioactivity of [carboxyl-^{14}C]-inulin in the lower chamber CPM/μl. The total clearance was calculated by summing up the clearance up to the specified time point. When the total clearance was plotted versus time, the slope estimated by linear regression analysis represents the permeability × surface area product. The PS value for the endothelial monolayer (PeS) was calculated as follows: $1/PeS = 1/P_{total}S - 1/P_{filter}S$, where $P_{total}S$ and $P_{filter}S$ are the PS values in the presence and absence of cells, respectively. The PeS value was divided by the surface area of the culture insert (0.3 cm^2) to give the endothelial permeability coefficient (Pe).

Western blot (WB) analysis

Cultured cells and human brain were homogenized in cell lysis buffer containing 10 mM Tris–HCl, pH 7.4, 1 mM EDTA, 1% Triton X-100, 0.1% sodium deoxycholate, 150 mM NaCl, and a protease inhibitor cocktail tablet (Roche, Basel, Switzerland). The homogenized sample was centrifuged at 5,000*g* for 10 min at 4°C and the supernatant was subjected to electrophoresis. Thirty micrograms of protein were mixed with an equal volume of Laemmli sample buffer (Bio-Rad Laboratories, Hercules, CA) containing 5% 2-mercaptoethanol and separated by electrophoresis on a 7% (*p*-gp) or a 10% (claudin-5 and SV40 large T-antigen) SDS–PAGE (Sigma) gel, followed by blotting onto polyvinylidene difluoride membranes. The membrane was blocked at room temperature for 2 h with 5% powdered skimmed milk in PBS containing 0.05% Tween 20 (PBS-T). The membrane was incubated with a primary antibody in PBS-T and 5% milk (1:500) at

TABLE 1. Human Primer Pairs Utilized in RT-PCR

Molecule	Sense	Antisense	Refs.
Occludin	5′-TGGGAGTGAACCCAACTGCT-3′	5′-CTTCAGGAACCGGCGTGGAT-3′	Ghassemifar et al. (2003)
Claudin-5	5′-CTGTTTCCATAGGCAGAGCG-3′	5′-AAGCAGATTCTTAGCCTTCC-3′	Varley et al. (2006)
JAM-A	5′-GACACGGGAAGACACTGGGACA-3′	5′-ATGCGCACAGCATTTGAAGTCA-3′	Ghassemifar et al. (2003)
ZO-1	5′-CATAGAATAGACTCCCCTGG-3′	5′-GCTTGAGGACTCGTATCTGT-3′	Ghassemifar et al. (2003)
ZO-2	5′-GCAGACTATCTGAGTTGCGACA-3′	5′-CTGGGCAATTTCGATCCTTGCA-3′	Ghassemifar et al. (2003)
GLUT-1	5′-TGTCCTATCTGAGCATCGTG-3′	5′-CTCCTCGGGTGTCTTATCAC-3′	Umeki et al. (2002)
CAT1	5′-TGGTGAGAAGTGGGTGAGGCT-3′	5′-GACCAGGACGTTAATACAAGTG-3′	Umeki et al. (2002)
LAT-1	5′-TCAAGCTCTGGATCGAGCTGCTC-3′	5′-TTCTGTAGGGGTTGATCATTTCC-3′	Umeki et al. (2002)
4F2hc	5′-CACAAGAACCAGAAGGATGA-3′	5′-ACTACCAGAAAACGCTCATT-3′	Dye et al. (2004)
MCT1	5′-GGGTGGGCAGTGGTAATTGGAGCT-3′	5′-GGCCCGATTGGTCGCATGAGGGCT-3′	Umeki et al. (2002)
CRT	5′-CCTCAGGTGTGGATAGATGC-3′	5′-GATGCCCATGCAGACCAGC-3′	Peral et al. (2002)
p-gp	5′-GCCTGGCAGCTGGAAGACAAATACACAAAATT-3′	5′-CAGACAGCAGCTGACAGTCCAAGAACAGGACT-3′	Weksler et al. (2005)
ABCG2	5′-TGGCTGTCATGGCTTCAGTA-3′	5′-GCCACGTGATTCTTCCACAA-3′	Weksler et al. (2005)
MRP1	5′-ACCAAGACGTATCAGGTGGCC-3′	5′-CTGTCTGGGCATCCAGGAT-3′	Weksler et al. (2005)
MRP2	5′-CCAATCTACTCTCACTTCAGCGAGA-3′	5′-AGATCCAGCTCAGGTCGGTACC-3′	Kusch-Poddar et al. (2005)
MRP4	5′-AAGTGAACAACCTCCAGTTCCA-3′	5′-CCGGAGCTTTCAGAATTGAC-3′	Kusch-Poddar et al. (2005)
MRP5	5′-AGTGGCACTGTCAGATCAAATT-3′	5′-TTGTTCTCTGCAGCAGCAAAC-3′	Weksler et al. (2005)
vWF	5′-CATTGGTGAGGATGGAGTCC-3′	5′-AGCACTGGTCTGCATTCTGG-3′	Fuchs et al. (2006)
G3PDH	5′-TGAAGGTCGGAGTCAACGGATTTGGT-3′	5′-CATGTGGGCCATGAGGTCCACCAC-3′	Ye et al. (2003)

room temperature for 2 h, followed by incubation with a secondary antibody in PBS-T and 5% milk (1:2,000) at room temperature for 1 h. The membranes were extensively washed in PBS-T and visualized by enhanced chemiluminescence detection (ECL-plus, Amersham, UK). A densitometric analysis using Quantity One (Bio-Rad Laboratories) was performed for quantification. HL60 cells, used as negative control cells that do not express claudin-5, were purchased from Japan Health Sciences Foundation. COS-7 cells were also obtained from the Japan Health Sciences Foundation.

Drug accumulation studies

Confluent TY08 cells grown in type I collagen-coated 24-well plates were washed three times with PBS and preincubated for 30 min at 37°C in a shaking water bath with or without the efflux transporter inhibitors: verapamil (100 μM), MK571 (10 μM), and novobiocin (300 μM). Next, the cells were incubated in culture medium containing the fluorescent substrates rhodamine 123 (10 μM), a substrate of *p*-gp and Breast Cancer Resistance Protein (BCRP), or calcein-AM (10 μM), a substrate of *p*-gp and multi-drug resistance-associated protein 1 (MRP1) with or without verapamil for an hour at 37°C. The cells were then washed three times with PBS and lysed in 1% Triton X-100. The amount of fluorescent substrates retained in the cells was detected using a MX3000P (Stratagene).

Results

Establishment of TY08 cell line

A conditionally immortalized HBMEC line, designated "TY08," was successfully generated using a retrovirus encoding a temperature-sensitive SV40 large T-antigen. TY08 cells were closely packed and exhibited contact inhibition at confluence (Fig. 1A). They showed a spindle-shaped morphology that has been well-defined in ECs constituting the BBB (Hosoya et al., 2000). One hundred percent of the cells were positive for DiI-Ac-LDL, indicating excellent purity (Fig. 1B). The endothelial origin of these cells was also supported by the detection of the factor VIII/vWF antigen mRNA (Fig. 1C) and protein (Fig. 1D). In order to demonstrate that the TY08 cells were truly contact inhibited under permissive temperatures as well as non-permissive temperatures, the cells in late passages (passage 13) were maintained at 33°C for 30 days (Fig. 1F) and the morphology of these cells was compared with that of the cells which had just become confluent (Fig. 1E). These results indicate that TY08 cells, even the late-passage cells, do not change their morphology, and continue to be truly contact inhibited. No change was detected in either the contact inhibition or the morphology from early passages to passage 15, which is the highest passage investigated so far (data not shown).

Temperature-sensitive nature of the TY08 cells

TY08 cells exhibited a robust proliferation at the permissive temperature of 33°C, with a doubling time of about 3 days (Fig. 2A). Two days after the temperature shift from 33 to 37°C, the cell growth was arrested (Fig. 2A). TY08 cells expressed large T-antigen with a molecular weight of 94 kDa, which is the same molecular weight as that in the COS-7 cells used as a positive control (Fig. 2B). Forty-eight hours after the temperature shift from 33 to 37°C, the amount of large

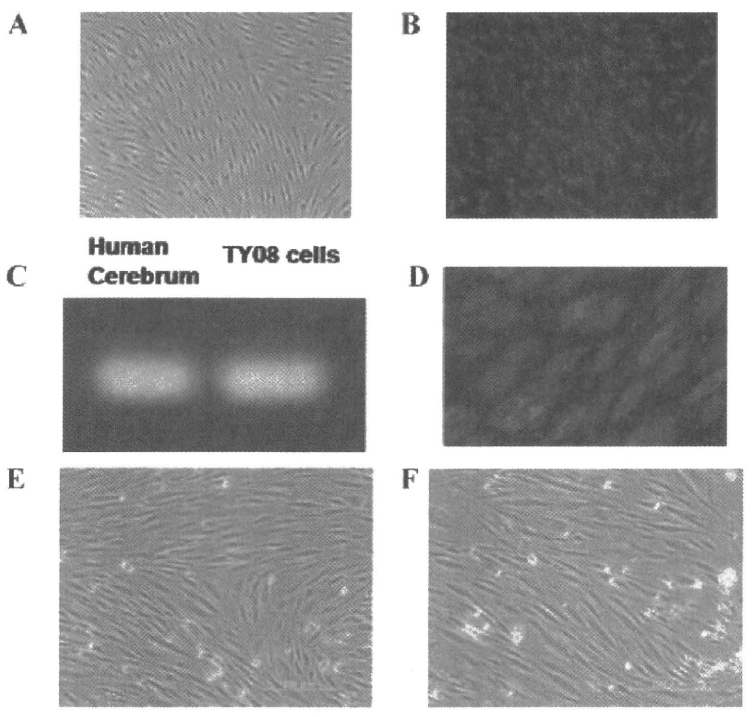

Fig. 1. The morphology and purity of TY08 cells. A: A phase contrast microscopic view of the TY08 cells (passage 7) demonstrates spindle-shaped morphology with contact inhibition. The cell proliferation continued to be contact-inhibited at 33°C even after the cells became confluent. B: All of the cells (passage 7) were positive for DiI-Ac-LDL, indicating that the purity of these endothelial cells is 100%. C: The expression of von Willebrand factor mRNA in TY08 cells (passage 7) was detected by RT-PCR. mRNAs from the human cerebrum were used as a positive control. D: Immunostaining of TY08 cells (passage 7) using an anti-von Willebrand factor antibody. E,F: The preservation of the contact inhibition of TY08 cells (passage 13) even 30 days after reaching the confluence at 33°C. TY08 cells (passage 13) that became confluent (E). Thirty days after the confluence (E), the same TY08 cells still showed contact inhibition under the permissive temperature of 33°C (F). [Color figure can be viewed in the online issue, which is available at wileyonlinelibrary.com.]

T-antigen in these cells decreased and the cells maintained lower expression for six successive days (Fig. 2B). The degradation assay for this protein was conducted within 24 h of the temperature shift to examine how fast tsA58 proteins in TY08 cells were degraded. Importantly, the amount of large T-antigen in the TY08 cells began to decrease within 30 min after the shift to the non-permissive temperature, and continued to decline in a time-dependent manner (Fig. 2C,D). Large T-antigen proteins were rapidly degraded at the non-permissive temperature of 37°C, and such a low level of this protein does not seem to be sufficient to immortalize the TY08 cells. Interestingly, there were no alterations in the morphology of the TY08 cells when they were compared at 1 and 24 h after the temperature shift from 33 to 37°C, irrespective of the quantity of large T-antigen protein (Fig. 2E,F). The TY08 cells grew stably over more than 14 passages when they were cultured at 33°C, retaining their spindle-shaped morphology (Fig. 2G). However, once the cells were seeded at 37°C, they gradually swelled and finally collapsed after about 14 days in culture, thus indicating "senescence" (Fig. 2G). In general, primary cultured HBMECs rapidly undergo senescence. These results show that TY08 cells grow stably as immortalized cells at the permissive temperature and show the phenotype of primary cultured HBMECs at the non-permissive temperature, indicating that the TY08 cells have an obvious temperature-sensitive nature, and can easily revert to ECs representative of those constituting the BBB of the human brain.

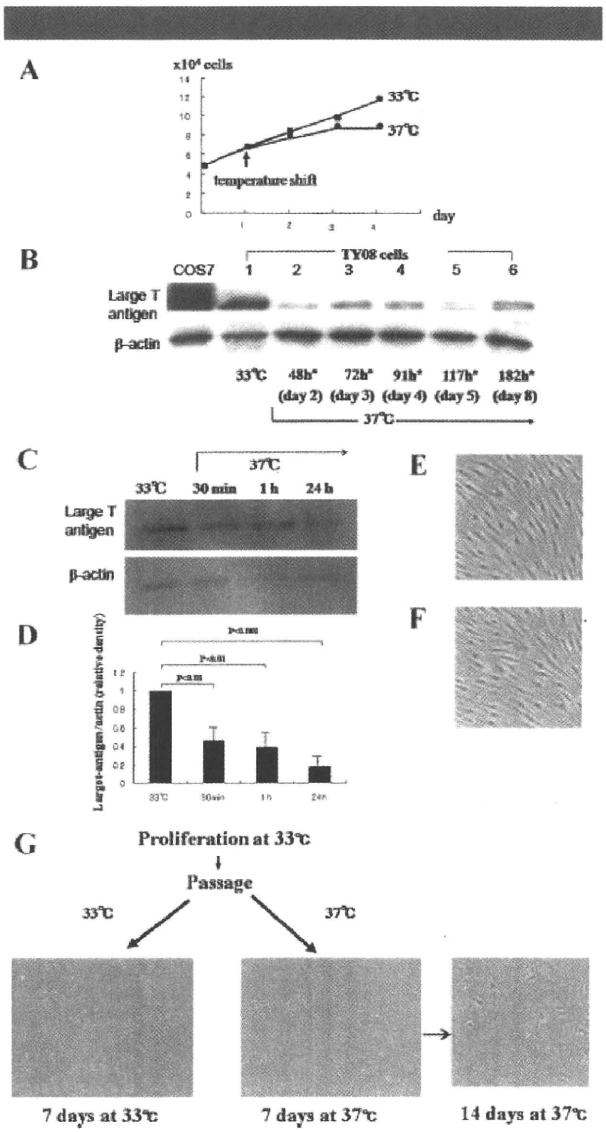

Fig. 2. The temperature-sensitive nature of the TY08 cells (passage 7). A: TY08 cells proliferated readily at the permissive temperature of 33°C. About 2 days after the temperature shift to 37°C, the cell growth was arrested. Each point represents the mean ± standard deviation (SD, n = 3). B: The quantity of tsA58 protein in the TY08 cells at the permissive or non-permissive temperature was examined using an anti-SV40 large T antigen antibody by WB. The tsA58 protein was detected as a dense and bold band in cells grown at 33°C. On the other hand, tsA58-proteins from cells grown under the non-permissive temperature of 37°C were thin and weak bands. No significant difference was observed between the quantity of protein expressed at 48 h after the temperature shift and that after 182 h. (*Time elapsed after the temperature shift from 33 to 37°C.) Three independent experiments were performed. C: After 30 min from the shift to 37°C, the amount of the protein in the TY08 cells began to decrease, and continued to decline until 24 h. Three independent experiments were performed; a result from one representative experiment is presented. D: Quantification of the Western blot data showed that the level of large T-antigen decreased progressively during the 24 h after the temperature shift to the non-permissive temperature. Three independent experiments were performed. The data are presented as the means and SD. E,F: TY08 cells did not show any alterations in their morphology 1 h (E) or 24 h (F) after the temperature shift from 33 to 37°C. G: TY08 cells return to a morphological state similar to the primary cultured parental endothelial cells derived from the BBB. This cell line shows robust proliferation under the permissive temperature from passage to passage, preserving their BBB-specific morphology. Once the cells were spread on the dish at 37°C, however, they gradually lost their proliferative ability and thereafter become swollen. As a result, they resemble the cells derived from the CNS that have not been immortalized. [Color figure can be viewed in the online issue, which is available at wileyonlinelibrary.com.]

Expression of tight junction molecules by the TY08 cells

Tight junctions between BMECs play a key role in the formation of the BBB, because TJs block the paracellular diffusion between ECs (Pardridge, 2005). Total RNA was isolated from the cells and processed for RT-PCR analysis to investigate the mRNA expression of the components of TJs in the TY08 cells. The expression of occludin, claudin-5, claudin-12, junctional adhesion molecule A (JAM-A), ZO-1, and ZO-2, corresponding to TJ components of ECs forming the BBB (Hawkins and Davis, 2005) was confirmed in the TY08 cells (Fig. 3A). Claudin-5 plays a key role in the barrier properties of brain capillary ECs (Nitta et al., 2003; Ohtsuki et al., 2007). Therefore, the expression of claudin-5 was investigated in the TY08 cells at the protein level by WB. As shown in Figure 3B, claudin-5 was detected by WB. The subcellular localization pattern of these TJ molecules was further investigated in the TY08 cells by immunohistochemical analyses. Besides claudin-5, occludin, ZO-1, and ZO-2 were also localized at the cell–cell boundaries in the TY08 cells (Fig. 3C–F). Six hours after the temperature shift from 33 to 37°C, at a time when the large T-antigen was considerably degraded, we evaluated the immunoreactivity of TJ proteins in TY08 cells. Not much difference was observed between the immunoreactivity of TJ proteins at 37°C and that at 33°C (data not shown).

Expression of transporters that can mediate influx in the TY08 cells

Brain microvascular ECs provide the blood-to-brain influx of various nutrients using influx transporters. The mRNA expression of various transporters that can mediate blood-to-brain influx in the TY08 cells was examined by RT-PCR analysis. Glucose transporter 1 (GLUT1), which takes in D-glucose from circulating blood (Cornford et al., 1994), was expressed in the TY08 cells (Fig. 4A). System L is a Na^+-independent large amino

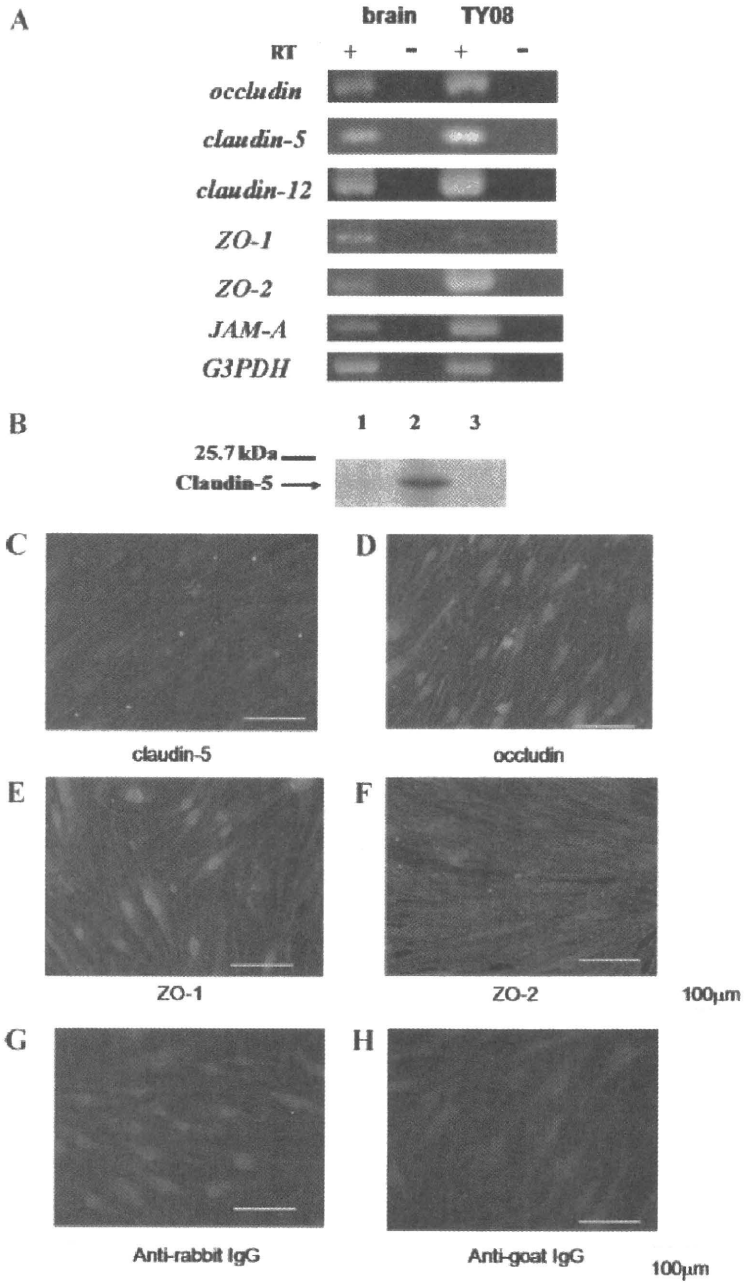

Fig. 3. The expression of tight junctional molecules by the TY08 cells (passage 7). A: The expression of occludin, claudin-5, claudin-12, ZO-1, ZO2, and JAM-A mRNA in a human brain tissue specimen and the TY08 cells were analyzed by PT-PCR. G3PDH was used as a control. Reactions were performed against total RNA with (+) or without (−) a reverse transcriptase (RT) reaction. B: Western blot analysis of claudin-5 in the TY08 cells. Claudin-5 was detected using an anti-claudin-5 antibody at the estimated molecular size (20 kDa). Lane 1, human cerebral cortex used as a positive control; lane 2, TY08 cells; lane 3, HL60, derived from leukemic cells and used as a negative control. Although a faint band was seen in the human cerebral cortex sample, a dense band was seen in the TY08 cells. No band was detected in the lysate from the HL60 cells. C–H: Immunocytochemical staining of tight junction proteins in confluent TY08 cells. Rabbit anti-claudin-5, rabbit anti-occludin, rabbit anti-ZO-1, and goat anti-ZO-2 antibodies were used as primary antibodies. Claudin-5 (C), occludin (D), ZO-1 (E), and ZO-2 (F), are known to play very important roles in maintaining TJs, and were all continuously detected at the cell–cell boundaries in the TY08 cells. No change was detected in the junctional expression of these proteins at passage 15 compared to earlier passages. FITC-conjugated anti-rabbit IgG antibodies were used as negative controls for claudin-5, occludin, and ZO-1 staining (G), and FITC-conjugated anti-goat IgG antibodies were used as a negative control for ZO-2 staining (H). Scale bars correspond to 100 μm.

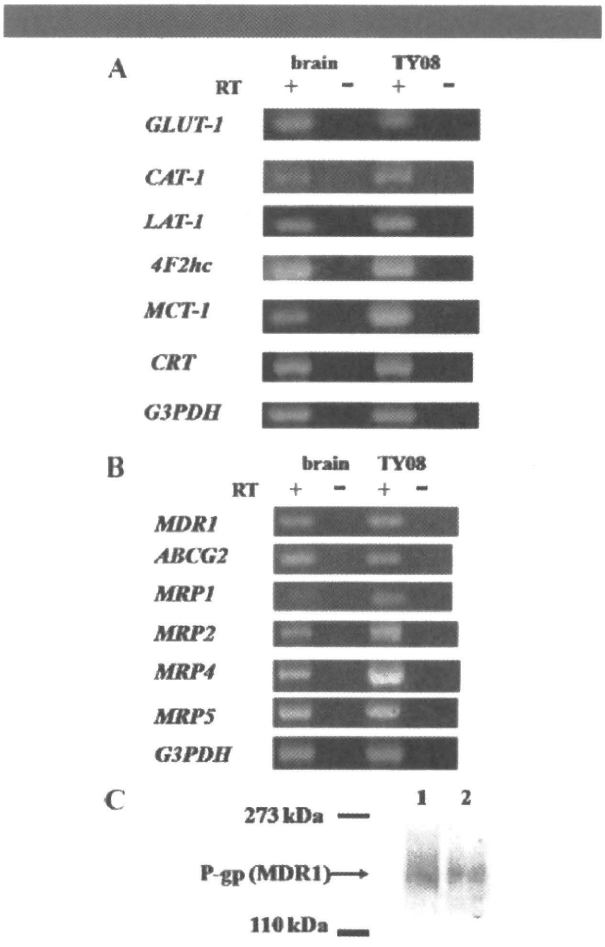

Fig. 4. The expression of transporters functioning at the BBB in the TY08 cells (passage 8). A: The expression of transporters that can mediate influx in the TY08 cells. The expression of GLUT-1, CAT-1, LAT-1, 4F2hc, MCT-1, and CRT mRNA in human brain and TY08 cells were examined. G3PDH was used as a control. Reactions were performed against total RNA with (+) or without (−) an RT reaction. B: The expression of blain-to-blood efflux transporters in the TY08 cells was also examined. The expression of MDR1 (*p*-gp), ABCG2 (BCRP), MRP1, MRP2, MRP4, and MRP5 mRNAs in human brain and TY08 cells was examined by RT-PCR. G3PDH was used as a control. Reactions were performed against total RNA with (+) or without (−) an RT reaction. C: Western blot analysis of *p*-gp in the TY08 cells using an anti-*p*-gp antibody; lane 1, human cerebral cortex used as a positive control; lane 2, TY08 cells. *p*-gp was detected at the estimated molecular size (170 kDa) in TY08 cells, as well as in the human brain tissue sample.

acid transport system present in the BBB, which transports large amino acids such as L-Tyr and also plays an important role in the delivery of L-dopa into the brain (Kanai et al., 1998). System L is composed of a heterodimer of the 4F2hc heavy chain and the LAT1 light chain (Kanai et al., 1998). LAT1 and 4F2hc mRNAs were amplified at their expected sizes, thus indicating that the TY08 cells express System L (Fig. 4A). System y^+ exists at the BBB and works as a Na^+-independent basic amino acid transport system which transports L-Lys and L-Arg (O'Kane et al., 2006). The cationic acid transporter 1 (CAT-1), which is responsible for system y^+ activity, was also expressed in the TY08 cells (Fig. 4A). Monocarboxylic acid transporter 1 (MCT1), which has been reported to work as a blood-to-brain transporter of monocarboxylic acids such as lactate (Kido et al., 2000), was also expressed in the TY08 cells (Fig. 4A). Creatine plays a pivotal role in the storage of phosphate-bound energy in the brain, and the creatine transporter (CRT) supplies creatine to the brain via the BBB (Ohtsuki et al., 2002). CRT was also expressed in the TY08 cells (Fig. 4A).

Expression of brain-to-blood efflux transporters in the TY08 cells

The BBB is also known to carry out the active efflux transport of various drugs and unnecessary metabolites from the brain to blood. The expression of various brain-to-blood efflux transporters was examined in the TY08 cells. Multidrug resistance gene 1a (Mdr1a), MRP1, MRP2, MRP4, MRP5, and ATP-binding cassette subfamily G member 2 (ABCG2), which are thought to mediate brain-to-blood efflux transport of diverse drugs at the BBB, were detected at the mRNA level in the TY08 cells (Fig. 4B). Among these brain-to-blood efflux transporters, *p*-gp, the translational product of MDR1a, was also detected at the protein level by WB (Fig. 4C).

The barrier function of the TY08 cells

The paracellular permeability to ions and low molecular weight molecules across the monolayer of the TY08 cells was assessed by measuring TEER and the permeability to inulin, respectively. The TEER of the TY08 cells was significantly higher than that of HUVECs and TR-BBBs, which lose their barrier activity due to a lack of claudin-5 (Ohtsuki et al., 2007; Fig. 5). The monolayers of the TY08 cells and TR-BBBs were also tested for the permeability to ^{14}C-inulin 30 min after the temperature shift from 33 to 37°C (Fig. 6). The Pe was determined to be 1.23×10^{-3} cm/min for TY08 cells and 4.75×10^{-3} cm/min for TR-BBBs. This Pe value of ^{14}C-inulin in the TY08 cells (1.23×10^{-3} cm/min) was as low as that of TR-BBB/CLD5 cells (1.14×10^{-3} cm/min), which have barrier properties through the exogenous expression of claudin-5 (Ohtsuki et al., 2007). These results indicate the possibility that the TY08 cells have functional TJs, and that these cells could thus be used for estimating the drug permeability across the human BBB.

Functional expression of *p*-glycoprotein in the TY08 cells

Next, the functionality of *p*-gp was examined in the TY08 cells at 37°C. The experiment was performed 30 min after the temperature shift when the large T-antigen was shown to have been considerably degraded. The influence of the *p*-gp inhibitor verapamil on the uptake of the *p*-gp substrates calcein-AM and rhodamine 123 in the TY08 cells was investigated. As shown in

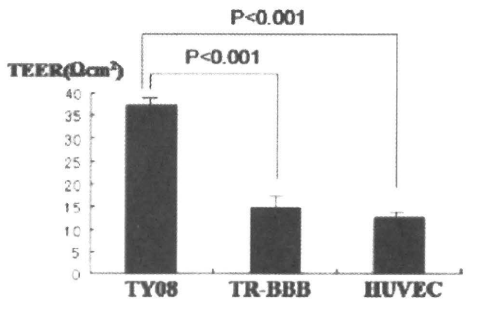

Fig. 5. TEER of the TY08 cells (passage 8). The TEER of the TY08 cells was significantly higher than that of TR-BBBs and HUVECs, which do not have barrier properties. The experiment was performed in triplicate. The data are presented as the means and SD.

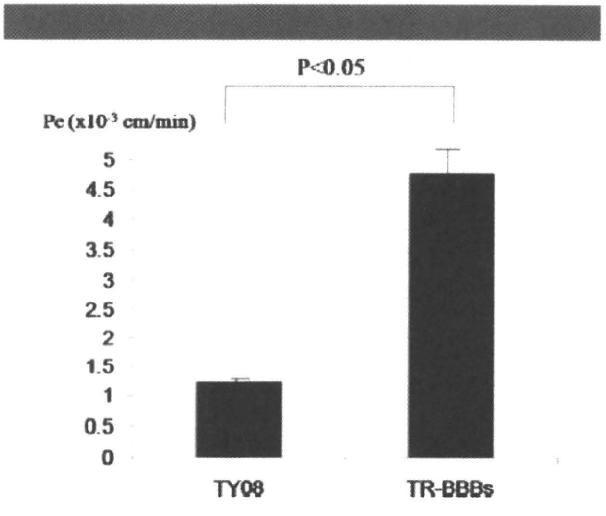

Fig. 6. Paracellular transport of ^{14}C inulin across monolayers of the TY08 cells (passage 9) and TR-BBBs. The permeability coefficients (Pe; mean ± SD, n = 3) of the endothelial monolayers are shown.

Figure 7, the inhibition of *p*-gp by verapamil led to a significantly increased uptake of calcein-AM (Fig. 7A) and rhodamine 123 (Fig. 7B), indicating that the *p*-gp expressed in the TY08 cells worked as an efflux pump against the *p*-gp substrates.

TY08 cells have superior barrier properties at the non-permissive temperature compared to the permissive temperature

To evaluate the barrier function of the TY08 cells at 37°C, we measured the TEER across the TY08 cells 14 h after the temperature shift from 33 to 37°C. The TEER values of the TY08 cells at 37°C were significantly higher than the control data from the TY08 cells that had been continuously incubated at 33°C (Fig. 8). These results indicate that the TY08 cells have superior barrier function at 37°C, the human physiological temperature, compared to 33°C.

Discussion

Cultured BMECs, so called "In vitro BBB models," can be a useful tool for studying the transport properties of the BBB and for analyzing the physiological and biological functions of the BBB. Primary cultured BMECs, in particular, HBMECs rapidly undergo senescence after a limited number of divisions (Stanimirovic et al., 1996). Hence, many of the in vitro BBB models reported so far have mostly been developed using immortalizing genes such as the SV40 large T-antigen gene. However, the SV40 large T-antigen interacts with numerous proteins, including retinoblastoma and p53, and these interactions often affect a wide variety of cellular functions (Terasaki et al., 2003). Therefore, the effect of large T-antigen has to be considered when using cells into which the large T-antigen gene has been introduced. In fact, one of the model cell lines immortalized by the SV40 large T-antigen did not show contact inhibition (i.e., they showed a tumor-like phenotype; Callahan et al., 2004). On the other hand, the conditionally immortalized BBB-derived ECs like TY08 can be used to analyze the BBB functions under conditions where T-antigen activity is reduced or absent, because the temperature-sensitive large T-antigen is degraded rapidly at 37°C. The most ideal in vitro human BBB model would consist of cells as close to primary HBMECs as possible, and these cells would exhibit robust proliferation in order to facilitate studies. To meet these requirements, the temperature-sensitive SV40 large T-antigen gene was used to establish the in vitro BBB model derived from human brain. The TY08 cells showed an obvious temperature-sensitive nature (Fig. 2), while maintaining contact inhibition for at least 30 days after becoming confluent, even under the permissive temperature of 33°C (Fig. 1E,F). These findings indicate that the TY08 cells did not gain any tumor-like phenotypes.

Failure of the TJs of the BBB is a critical event in the development and progression of several diseases that affect the central nervous system (CNS), including multiple sclerosis (Plumb et al., 2002), cerebral ischemia (Fischer et al., 2004), and

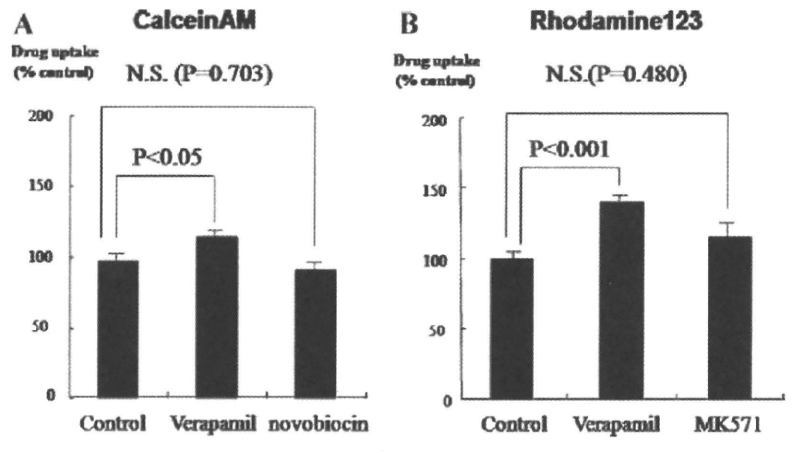

Fig. 7. Functionality of *p*-gp expressed by TY08 cells (passage 8). The cellular uptake of calcein-AM (A) and rhodamine 123 (B) was measured in the presence or absence of verapamil, a specific inhibitor of *p*-gp. A: Calcein-AM is a substrate of *p*-gp and MRP-1. The uptake of calcein-AM in the presence of verapamil was significantly higher than that of controls without verapamil. On the other hand, the uptake of calcein-AM in the presence of novobiocin, a specific inhibitor of BCRP, did not show a significant change. B: Rhodamine 123 is a substrate of both *p*-gp and BCRP. While the uptake of rhodamine 123 was not significantly influenced by MK571, a specific inhibitor of MRP-1, verapamil significantly increased the uptake of rhodamine 123 by the TY08 cells. The experiment was performed in triplicate. The data are presented as the means and SD.

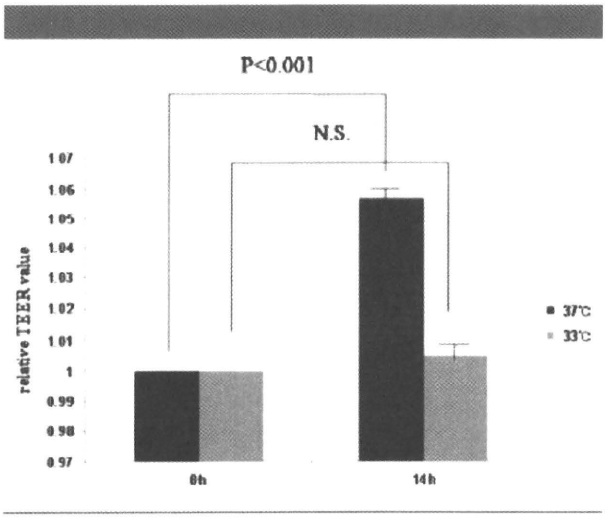

Fig. 8. TY08 cells (passage 8) cultured under the non-permissive temperature have higher TEER values than the cells grown at 33°C. After becoming confluent at 33°C (TEER values were 35–40 Ωcm^2), the cell culture inserts with TY08 cells were transferred into an incubator which was set to 37°C. Fourteen hours after the temperature shift, the TEER values across the TY08 cells were measured (N = 5). As controls, the TEER values of the TY08 cells which were continuously incubated at 33°C were also measured (N = 5). The data are presented as the means and SD.

Alzheimer's disease (Chen et al., 2008). Several proteins have been reported to be localized at TJs, including occludin (Furuse et al., 1993), claudin-5 (Nitta et al., 2003), claudin-12 (Nitta et al., 2003; Ohtsuki et al., 2007), ZO-1, ZO-2 (Biernacki et al., 2004), and JAM-A (Yeung et al., 2008). The TY08 cells developed in our laboratory expressed all of these molecules important for maintaining functional TJs. In addition, TY08 cells displayed a junctional expression of claudin-5, occludin, ZO-1, and ZO-2. Importantly, occludin is highly expressed and consistently presents in a distinct, continuous pattern along the cell margins in the cerebral endothelium (Hawkins et al., 2004), whereas it is much more sparsely distributed in non-neural ECs (Hirase et al., 1997). The TY08 cells displayed a distinct, continuous expression of this TJ protein (Fig. 3D). Nitta et al. (2003) reported size-selective opening of the BBB in claudin-5-deficient mice. Ohtsuki et al. (2007) also reported that exogenous expression of claudin-5 induces barrier properties in cultured rat brain capillary ECs. Notably, the expression of claudin-5 in the TY08 cells was demonstrated not only by immunohistochemistry but also by WB. These results indicated that TY08 cells represent a useful tool for analyzing the pathological mechanisms underlying TJ dysfunction at the molecular level.

The BBB expresses various influx and efflux transporters that play roles not only in supplying nutrients but also in excluding drugs and excessive neurotoxic materials such as neurotransmitters and their metabolites. The expression of representative transporters that can mediate influx was observed in the TY08 cells by RT-PCR. TY08 is the first in vitro BBB model derived from human brain that expresses so many different influx transporters. We also examined the expression of representative brain-to-blood efflux transporters by the TY08 cells. Among the most significant efflux transporters at the BBB are *p*-gp (Schinkel et al., 1996), MRPs (Nies et al., 2004), and ABCG2 (Cisternino et al., 2004), all of which are thought to prevent xenobiotics from entering the CNS. TY08 cells expressed ABCG2, MRP1, MRP2, MRP4, and MRP5, as well as *p*-gp. In addition, the functional expression of *p*-gp, which is the most studied efflux transporter on the BBB, and has also been shown to play a crucial role for protecting the brain from various neurotoxic agents, was shown in the TY08 cells. Interestingly, *p*-gp is involved in the brain-to-blood excretion of Aβ peptides, and it has been suggested that the protein might be involved in the development of Alzheimer's disease (Cirrito et al., 2005). Taken together, these results suggest that TY08 cells might be a useful tool not only for estimating drug permeability across the BBB, but also for developing new therapeutic strategies against Alzheimer's disease.

The TEER value found in TY08 cells was relatively low (35–43 Ωcm^2) despite the fact that this value was significantly higher than that of the negative control cells (HUVECs and TR-BBBs). However, the TEER of hCMEC/D3, which has been recently reported and fully characterized to be an immortalized human in vitro BBB model, was also reported to have low values (30–40 Ωcm^2; Weksler et al., 2005). In contrast, bovine BMEC monolayers reach a TEER above 500 Ωcm^2 (Deri et al., 2005). Taking into account the evidence shown in hCMEC/D3 and TY08 cells, both of which have been proven to maintain many of the in vivo BBB functions, the TEER value of the ECs derived from the human brain without the support of astrocytes or other helpful factors such as cAMP might be lower than that of the endothelium from animals such as a cow. Co-culture with astrocytes in the presence or absence of cAMP-inducing agents, conditions which have been documented to reduce the passive permeability of cultured BMECs (Perrière et al., 2007), will need to be investigated with TY08 monolayers.

In conclusion, a conditionally immortalized in vitro BBB model derived from human brain, which maintains most of the in vivo BBB properties, was successfully established. This cell line, designated "TY08", might therefore be a useful tool for the development of new therapeutic methods against the many CNS disorders, including cerebral ischemia, multiple sclerosis, and Alzheimer's disease.

Acknowledgments

This study was supported in part by research grants (No. 18390259 and 19790610) from the Japan Society for the Promotion of Science, Tokyo, Japan.

Literature Cited

Biernacki K, Prat A, Blain M, Antel JP. 2004. Regulation of cellular and molecular trafficking across human brain endothelial cells by Th1- and Th2-polarized lymphocytes. J Neuropathol Exp Neurol 63:223–232.

Callahan MK, Williams KA, Kivisäkk P, Pearce D, Stins MF, Ransohoff RM. 2004. CXCR3 marks CD4+ memory T lymphocytes that are competent to migrate across a human brain microvascular endothelial cell layer. J Neuroimmunol 153:150–157.

Chen X, Gawryluk JW, Wagener JF, Ghribi O, Geiger JD. 2008. Caffeine blocks disruption of blood brain barrier in a rabbit model of Alzheimer's disease. J Neuroinflammation 5:12–25.

Cirrito JR, Deane R, Fagan AM, Spinner ML, Parsadanian M, Finn MB, Jiang H, Prior JL, Sagare A, Bales KR, Paul SM, Zlokovic BV, Piwnica-Worms D, Holtzman DM. 2005. *P*-glycoprotein deficiency at the blood–brain barrier increases amyloid-beta deposition in an Alzheimer disease mouse model. J Clin Invest 115:3285–3290.

Cisternino S, Mercier C, Bourasset F, Roux F, Scherrmann JM. 2004. Expression, up-regulation, and transport activity of the multidrug-resistance protein Abcg2 at the mouse blood–brain barrier. Cancer Res 64:3296–3301.

Cornford EM, Hyman S, Swartz BE. 1994. The human brain GLUT1 glucose transporter: Ultrastructural localization to the blood–brain barrier endothelia. J Cereb Blood Flow Metab 14:106–112.

Deri MA, Abraham CS, Kataoka Y, Niwa M. 2005. Permeability studies on in vitro blood–brain barrier models: physiology, pathology, and pharmacology. Cell Mol Neurobiol 25:59–127.

Dye JF, Vause S, Johnston T, Clark P, Firth JA, D'Souza SW, Sibley CP, Glazier JD. 2004. Characterization of cationic amino acid transporters and expression of endothelial nitric oxide synthase in human placental microvascular endothelial cells. FASEB J 18:125–127.

Fischer S, Wiesnet M, Marti HH, Renz D, Schaper W. 2004. Simultaneous activation of several second messengers in hypoxia-induced hyperpermeability of brain derived endothelial cells. J Cell Physiol 198:359–369.

Fuchs S, Hermanns MI, Kirkpatrick CJ. 2006. Retention of a differentiated endothelial phenotype by outgrowth endothelial cells isolated from human peripheral blood and expanded in long-term cultures. Cell Tissue Res 326:79–92.

Furuse M, Hirase T, Itoh M, Nagafuchi A, Yonemura S, Tsukita S, Tsukita S. 1993. Occludin: A novel integral membrane protein localizing at tight junctions. J Cell Biol 123:1777–1788.

Ghassemifar MR, Eckert JJ, Houghton FD, Picton HM, Leese HJ, Fleming TP. 2003. Gene expression regulating epithelial intercellular junction biogenesis during human blastocyst development in vitro. Mol Hum Reprod 9:245–252.

Hawkins BT, Davis TP. 2005. The blood–brain barrier/neurovascular unit in health and disease. Phamacol Rev 57:173–185.

Hawkins BT, Abbruscato TJ, Egleton RD, Brown RC, Huber JD, Campos CR, Davis TP. 2004. Nicotine increases in vivo blood–brain barrier permeability and alters cerebral microvascular tight junction protein distribution. Brain Res 1027:48–58.

Hirase T, Staddon JM, Saitou M, Ando-Akatsuka Y, Itoh M, Furuse M, Fujimoto K, Tsukita S, Rubin LL. 1997. Occludin as a possible determinant of tight junction permeability in endothelial cells. J Cell Sci 110:1603–1613.

Hosoya K, Takashima T, Tetsuka K, Nagura T, Ohtsuki S, Takanaga H, Ueda M, Yanai N, Obinata M, Terasaki T. 2000. mRNA expression and transport characterization of conditionally immortalized rat brain capillary endothelial cell lines; a new in vitro BBB model for drug targeting. J Drug Target 8:357–370.

Jat PS, Sharp PA. 1989. Cell lines established by a temperature-sensitive simian virus 40 large-T-antigen gene are growth restricted at the nonpermissive temperature. Mol Cell Biol 9:1672–1681.

Joó F. 1996. Endothelial cells of the brain and other systems: Some similarities and differences. Prog Neurobiol 48:255–273.

Kanai Y, Segawa H, Miyamoto K, Uchino H, Takeda E, Endou H. 1998. Expression cloning and characterization of a transporter for large neutral amino acids activated by the heavy chain of 4F2 antigen (CD98). J Biol Chem 273:23629–23632.

Kanda T, Yoshino H, Ariga T, Yamawaki M, Yu RK. 1994. Glycosphingolipid antigens in cultured microvascular bovine brain endothelial cells: Sulfoglucuronosyl paragloboside as a target of monoclonal IgM in demyelinative neuropathy. J Cell Biol 126:235–246.

Ketabi-Kiyanvash N, Herold-Mende C, Kashfi F, Caldeira S, Tommasino M, Haefeli WE, Weiss J. 2007. NKIM-6, a new immortalized human brain capillary endothelial cell line with conserved endothelial characteristics. Cell Tissue Res 328:19–29.

Kido Y, Tamai I, Okamoto M, Suzuki F, Tsuji A. 2000. Functional clarification of MCT1-mediated transport of monocarboxylic acids at the blood–brain barrier using in vitro cultured cells and in vivo BUI studies. Pharm Res 17:55–62.

Kusch-Poddar M, Drewe J, Fux I, Gutmann H. 2005. Evaluation of the immortalized human brain capillary endothelial cell line BB19 as a human cell culture model for the blood–brain barrier. Brain Res 1064:21–31.

Muruganandam A, Herx LM, Monette R, Durkin JP, Stanimirovic DB. 1997. Development of immortalized human cerebromicrovascular endothelial cell line as an in vitro model of the human blood–brain barrier. FASEB J 11:1187–1197.

Nies AT, Jedlitschky G, König J, Herold-Mende C, Steiner HH, Schmitt HP, Keppler D. 2004. Expression and immunolocalization of the multidrug resistance proteins, MRP1-MRP6 (ABCC1-ABCC6), in human brain. Neuroscience 129:349–360.

Nitta T, Hata M, Gotoh S, Seo Y, Sasaki H, Hashimoto N, Furuse M, Tsukita S. 2003. Size-selective loosening of the blood–brain barrier in claudin-5-deficient mice. J Cell Biol 161:653–660.

Ohtsuki S, Tachikawa M, Takanaga H, Shimizu H, Watanabe M, Hosoya K, Terasaki T. 2002. The blood–brain barrier creatine transporter is a major pathway for supplying creatine to the brain. J Cereb Blood Flow Metab 22:1327–1335.

Ohtsuki S, Sato S, Yamaguchi H, Kamoi M, Asashima T, Terasaki T. 2007. Exogenous expression of claudin-5 induces barrier properties in cultured rat brain capillary endothelial cells. J Cell Physiol 210:81–86.

O'Kane RL, Viña JR, Simpson I, Zaragozá R, Mokashi A, Hawkins RA. 2006. Cationic amino acid transport across the blood–brain barrier is mediated exclusively by system y+. Am J Physiol Endocrinol Metab 291:E412–E419.

Pardridge WM. 2005. The blood–brain barrier: Bottleneck in brain drug development. NeuroRx 2:3–14.

Peral MJ, García-Delgado M, Calonge ML, Durán JM, De La Horra MC, Wallimann T, Speer O, Ilundáin A. 2002. Human, rat and chicken small intestinal Na^+- and Cl^--creatine transporter: Functional, molecular characterization and localization. J Physiol 545:133–144.

Perrière N, Yousif S, Cazaubon S, Chaverot N, Bourasset F, Cisternino S, Declèves X, Hori S, Terasaki T, Deli M, Scherrmann JM, Temsamani J, Roux F, Couraud PO. 2007. A functional in vitro model of rat blood–brain barrier for molecular analysis of efflux transporters. Brain Res 1150:1–13.

Plumb J, McQuaid S, Mirakhur M, Kirk J. 2002. Abnormal endothelial tight junctions in active lesions and normal-appearing white matter in multiple sclerosis. Brain Pathol 12:154–169.

Schinkel AH, Wagenaar E, Mol CA, van Deemter L. 1996. *P*-glycoprotein in the blood–brain barrier of mice influences the brain penetration and pharmacological activity of many drugs. J Clin Invest 97:2517–2524.

Stanimirovic D, Morley P, Ball R, Hamel E, Mealing G, Durkin JP. 1996. Angiotensin II-induced fluid phase endocytosis in human cerebromicrovascular endothelial cells is regulated by the inositol-phosphate signaling pathway. J Cell Physiol 169:455–467.

Terasaki T, Ohtsuki S, Hori S, Takanaga H, Nakashima E, Hosoya K. 2003. New approaches to in vitro models of blood–brain barrier drug transport. Drug Discov Today 8:944–954.

Umeki N, Fukasawa Y, Ohtsuki S, Hori S, Watanabe Y, Kohno Y, Terasaki T. 2002. mRNA expression and amino acid transport characteristics of cultured human brain microvascular endothelial cells (hBME). Drug Metab Pharmacokinet 17:367–373.

Varley CL, Garthwaite MA, Cross W, Hinley J, Trejdosiewicz LK, Southgate J. 2006. PPARgamma-regulated tight junction development during human urothelial cytodifferentiation. J Cell Physiol 208:407–417.

Weksler BB, Subileau EA, Perrière N, Charneau P, Holloway K, Leveque M, Tricoire-Leignel H, Nicotra A, Bourdoulous S, Turowski P, Male DK, Roux F, Greenwood J, Romero IA, Couraud PO. 2005. Blood–brain barrier-specific properties of a human adult brain endothelial cell line. FASEB J 19:1872–1874.

Ye L, Martin TA, Parr C, Harrison GM, Mansel RE, Jiang WG. 2003. Biphasic effects of 17-beta-estradiol on expression of occludin and transendothelial resistance and paracellular permeability in human vascular endothelial cells. J Cell Physiol 196:362–369.

Yeung D, Manias JL, Stewart DJ, Nag S. 2008. Decreased junctional adhesion molecule-A expression during blood–brain barrier breakdown. Acta Neuropathol 115:635–642.

Journal of Cellular Physiology

Peripheral Nerve Pericytes Modify the Blood–Nerve Barrier Function and Tight Junctional Molecules Through the Secretion of Various Soluble Factors

FUMITAKA SHIMIZU,[1] YASUTERU SANO,[1] MASA-AKI ABE,[1] TOSHIHIKO MAEDA,[1] SUMIO OHTSUKI,[2] TETSUYA TERASAKI,[2] AND TAKASHI KANDA[1]*

[1]*Department of Neurology and Clinical Neuroscience, Yamaguchi University Graduate School of Medicine, Ube, Japan*

[2]*Department of Molecular Biopharmacy and Genetics, Graduate School of Pharmaceutical Sciences, Tohoku University, Sendai, Japan*

The objectives of this study were to establish pure blood–nerve barrier (BNB) and blood–brain barrier (BBB)-derived pericyte cell lines of human origin and to investigate their unique properties as barrier-forming cells. Brain and peripheral nerve pericyte cell lines were established via transfection with retrovirus vectors incorporating human temperature-sensitive SV40 T antigen (*tsA58*) and telomerase. These cell lines expressed several pericyte markers such as α-smooth muscle actin, NG2, platelet-derived growth factor receptor β, whereas they did not express endothelial cell markers such as vWF and PECAM. In addition, the inulin clearance was significantly lowered in peripheral nerve microvascular endothelial cells (PnMECs) through the up-regulation of claudin-5 by soluble factors released from brain or peripheral nerve pericytes. In particular, bFGF secreted from peripheral nerve pericytes strengthened the barrier function of the BNB by increasing the expression of claudin-5. Peripheral nerve pericytes may regulate the barrier function of the BNB, because the BNB does not contain cells equivalent to astrocytes which regulate the BBB function. Furthermore, these cell lines expressed several neurotrophic factors such as NGF, BDNF, and GDNF. The secretion of these growth factors from peripheral nerve pericytes might facilitate axonal regeneration in peripheral neuropathy. Investigation of the characteristics of peripheral nerve pericytes may provide novel strategies for modifying BNB functions and promoting peripheral nerve regeneration.

J. Cell. Physiol. 226: 255–266, 2010.

Brain and peripheral nerve pericytes, which completely surround capillary endothelial cells, are the critical components of the blood–brain barrier (BBB) and blood–nerve barrier (BNB). Pericytes play important roles in mediating the development, maintenance, and regulation of the BBB and BNB. Pericytes may contribute to the regulation of BBB and BNB–endothelial function by paracrine secretion of growth factors such as Ang 1 (Davis et al., 1996), TGF-β (Sato and Rifkin, 1989; Hirschi et al., 2003), VEGF (Brown et al., 2001; Reinmuth et al., 2001), and bFGF (Niimi, 2003). In addition, extensive pericyte coverage is found around microvessels in organs that have a barrier system, and the pericyte-to-endothelial ratios are 1:1 in the retina and brain and approximately 1:10 in the lung (Shepro and Morel, 1993). It is not clear why the nervous system requires a larger degree of pericyte coverage than other organs, but one possibility is that brain and peripheral nerve pericytes contribute to the regulation of the BBB and BNB and increase vascular stability.

The loss of pericytes from the microvasculature is one of the earliest hallmarks of several angiopathy-related diseases. Pericyte loss from microvessels is associated with the formation of microaneurysms, microhemorrhage, and local edema in diabetic microangiopathy (Giannini and Dyck, 1995; Lindahl et al., 1997; Hammes, 2005). CADASIL, which is an increasingly recognized autosomal-dominant vascular dementia caused by highly stereotyped mutations in the Notch3 receptor, is a widespread angiopathy characterized by pericyte degeneration. Therefore, clarifying the molecular mechanisms by which pericytes regulate BBB and BNB functions under both physiological and pathological conditions would positively contribute to the development of a novel therapy for many vessel-related diseases such as diabetic microangiopathy and stroke.

Primary cultures of retinal and brain pericytes derived from rat, bovine, and human tissue have been used for in vitro investigation of the physiological roles of pericytes (Capetandes and Gerritsen, 1990; Kondo et al., 2003). Although endoneurial pericytes would be useful sources for investigating the roles of pericytes in pathological conditions such as diabetic neuropathy, no optimal pericyte cell lines originating from the BNB have been developed. This absence is partly due to the difficulty in isolating a sufficient amount of pericytes from a miniscule amount of endoneurial tissue. Recently, brain and peripheral nerve pericyte cell lines were successfully established from rats (Shimizu et al., 2008). However, brain and peripheral nerve pericytes of human tissue origin are definitely necessary in order to study human BBB and BNB function.

The purpose of the present study was to establish pure BBB- and BNB-derived pericyte cell lines from human tissue

Contract grant sponsor: Ministry of Health, Labor and Welfare of Japan.
Contract grant sponsor: Japan Society for the Promotion of Science, Tokyo, Japan;
Contract grant number: 22790821.

*Correspondence to: Takashi Kanda, Department of Neurology and Clinical Neuroscience, Yamaguchi University Graduate School of Medicine, 1-1-1, Minami-kogushi, Ube, Yamaguchi 755-8505, Japan. E-mail: tkanda@yamaguchi-u.ac.jp

Received 16 March 2010; Accepted 7 July 2010

Published online in Wiley Online Library (wileyonlinelibrary.com.), 27 July 2010.
DOI: 10.1002/jcp.22337

origin by transfection with retrovirus vectors incorporating human temperature-sensitive SV40 T antigen (*tsA58*) and human telomerase (*hTERT*) and to characterize the established pericyte cell lines. In addition, the differences of cellular properties between brain pericytes originating from the BBB were compared with peripheral nerve pericytes originating from the BNB. In addition, these cell lines up-regulated the barrier function of endothelial cells in the BBB and BNB.

Materials and Methods

Reagents

The culture medium for pericytes was Dulbecco's modified Eagle's medium (DMEM; Sigma, St. Louis, MO) containing 100 U/ml penicillin (Sigma), 100 μg/ml streptomycin (Sigma), 25 ng/ml amphotericin B (Invitrogen, Grand Island, NY), and 10% fetal bovine serum (FBS; Sigma). Polyclonal anti-NG2, anti-Ang-1, anti-BDNF, and anti-GDNF antibodies were obtained from Santa Cruz (Santa Cruz, CA). Monoclonal anti-SV40 antibody was purchased from Calbiochem (Darmstadt, Germany). Monoclonal anti-SMA antibody and polyclonal anti-vWF antibody were obtained from Dako (A/S,Glostrup, Denmark). Polyclonal anti-claudin-5 and anti-occludin antibodies were purchased from Zymed (San Francisco, California). Polyclonal anti-bFGF, anti-TGF-β, and anti-VEGF antibodies were purchased from R&D Systems (Minneapolis, Minnesota). Recombinant human TGF-β, Ang-1, VEGF, bFGF, and TNF-α were purchased from Peprotech EC (London, UK). Human umbilical vein ECs (HUVEC) and HL-60 cells were obtained from Japan Health Sciences Foundation (Osaka, Japan), and human astrocytes were purchased from Lonza (Walkersville, Maryland). TY10 cells were conditionally immortalized a brain microcapillary endothelial cell line (BMECs) (Sano et al., 2010), and used as in vitro BBB model. Primary human fibroblasts were obtained from DS Pharma Biomedical (Osaka, Japan).

Isolation of peripheral nerve and brain pericytes and establishment of cell lines

The study protocol for human tissue was approved by the ethics committee of the Medical Faculty, University of Yamaguchi Graduate School and was conducted in accordance with the Declaration of Helsinki, as amended in Somerset West in 1996. Written informed consent was obtained from the family of the participants before entering the study.

Human sciatic nerve and brain tissues samples were obtained from a patient who suddenly died from a heart attack. The isolation procedure follows that of the previous method with modification (Kanda et al., 1997). Briefly, the sciatic nerve was removed and the endoneurium was carefully separated from the epineurium and perineurium using fine forceps, dissected into small pieces, and digested with 0.25% type I collagenase (Sigma). After centrifugation, the mixture was centrifuged, and the pellet was suspended in 15% dextran solution. The pellet was resuspended and cell suspension placed onto a type I collagen-coated dish (Becton Dickinson, Tokyo, Japan). The brain capillary-rich fractions were isolated using a previously reported method (Kanda et al., 1994). Briefly, the cerebral cortex of the human brain was homogenized, and the homogenate was further dissociated with 0.005% dispase (Sigma). After the mixture was centrifuged, the pellet was suspended in 15% dextran solution. Next, the pellet was resuspended and the cell suspension was filtered through a 190-μm nylon mesh, and the filtered cell clusters were plated onto a type I collagen-coated dish. The colonies of pericyte and peripheral nerve microvascular endothelial cells (PnMECs) were isolated using a cloning cap. Pure peripheral nerve and brain pericytes, and PnMECs were isolated after two or three passages. Thereafter, peripheral nerve and brain pericytes were immortalized via sequential transduction with retrovirus-incorporated *tsA58* and *hTERT* genes. Pericytes were initially incubated overnight with a high concentration of retrovirus vector carrying *tsA58* in 10% DMEM. The cells were subsequently washed, and the temperature was adjusted from 37 to 33°C to activate the large T-antigen. This process was followed by another overnight incubation with a high concentration of retrovirus vector carrying *hTERT*.

Reverse transcription-polymerase chain reaction (RT-PCR) analysis

Total RNA was extracted using an RNeasy® Plus Mini Kit (Qiagen, Hilden, Germany) following the manufacturer's protocol. Single-stranded cDNA was created from 40 ng total RNA by StrataScript First Strand Synthesis System (Stratagene®, Cedar Greek, TX). The sequence specificity of each human primer pair and its reference are shown in Table 1. RT-PCR amplification was performed using TAKARA PCR Thermal Cycler Dice (Takara, Otsu, Japan). The RT-PCR amplification products were separated by electrophoresis in 2% agarose gels containing 0.5 mg/ml ethidium bromide and visualized with an imager.

Quantitative real-time PCR analysis

A quantitative real-time PCR analysis was performed using a Stratagene's Mx3005P (Stratagene®) with FullVelocity® SYBR® Green QPCR master mix (Stratagene®) according to the manufacturer's protocol. The sequences of primers are shown in Table 1. Glyceraldehyde-3-phosphate dehydrogenase (GAPDH) was used as an internal standard. The samples were subjected to PCR analysis using the following cycling parameters: 95°C for 10 min, 95°C for 15 sec, and 60°C for 1 min for 40 cycles. Negative controls (cDNA-free solutions) were included in each reaction. The standard reaction curve was analyzed by MxPro™ (Stratagene®) software and the relative quantity according to standard reaction curve (R_v) was calculated according to the formula $R_v = R_{Gene}/R_{GAPDH}$ by computer.

TABLE 1. Human primer pairs utilized in RT-PCR analysis

Target	Sense	Antisense	Refs.
PDGF-β	5′-AATGTCTCCAGCACCTTCGT-3′	5′-AGCGGATGTGGTAAGGCATA-3′	Basciani et al. (2002)
Osteopontin	5′-ACCCTCTCTGACACCCTGTG-3′	5′-GGCTGGCTTCTCACATTCTC-3′	Said et al. (2007)
Ang-1	5′-GGAAGTCTAGATTTCCAAAGAGGC-3′	5′-CTTTATCCCATTCAGTTTTCCATG-3′	Huang et al. (2000)
TGF-β1	5′-ACCAACTATTGCTTCAGCTC-3′	5′-TTATGCTGGTTGTACAGG-3′	Soufla et al. (2005)
VEGF	5′-GCAGAAGGAGGAGGGCAGAATC-3′	5′-ACACTCCAGGCCCTCGTCATT-3′	Soufla et al. (2005)
BFGF	5′-GAAGAGCGACCCTCACATCAAG-3′	5′-CTGCCCAGTTCGTTTCAGTG-3′	Soufla et al. (2005)
NGF	5′-TCATCATCCCATCCCATCTT-3′	5′-CTTGACAAAGGTGTGAGTCG-3′	Bronzetti et al. (2006)
BDNF	5′-AGCCTCCTCTGCTCTTTCTGCTGGA-3′	5′-CTTTTGTCTATGCCCCTGCAGCCTT-3′	Bronzetti et al. (2006)
GDNF	5′-CGCCGCCGGACGGGACTTTAAGATGAAGTTA-3′	5′-CAAGAGCCGCTGCAGTACCTAAAAATCA-3′	Bäckman et al. (2006)
VWF	5′-CACCATTCAGCTAAGAGGAGG-3′	5′-GCCCTGGCAGTAGTGGATA-3′	Fuchs et al. (2006)
Claudin-5	5′-CTGTTTCCATAGGCAGAGCG-3′	5′-AAGCAGATTCTTAGCCTTCC-3′	Varley et al. (2006)
Occludin	5′-TGGGAGTGAACCCAACTGCT-3′	5′-CTTCAGGAACCGGCGTGGAT-3′	Ghassemifar et al. (2003)
G3PDH	5′-TGAAGGTCGGAGTCAACGGATTTGGT-3′	5′-CATGTGGGCCATGAGGTCCACCAC-3′	Ye (2003)
GAPDH (real-time)	5′-GTCAA CGGAT TTGGT CTGTA TT-3′	5′-AGTCT TCTGG GTGGC AGTGAT-3′	Zhang et al. (2006)

Western blot analysis

The proteins samples (10–20 μg) were separated by SDS–PAGE (Biorad, Tokyo, Japan), and transferred to nitrocellulose membrane (Amersham, Chalfont, UK). The membranes were treated with blocking buffer (5% skimmed milk in 25 mM Tris–HCl, pH 7.6, 125 nM NaCl, 0.5% Tween-20) for 1 h at room temperature and incubated with relevant antibodies (dilution 1:100) for 2 h at room temperature as the primary antibodies. The membrane were exposed to peroxidase-conjugated secondary antibody (1:2,000) followed by chemiluminescence reagent (Amersham), exposure to X-Omat S films (Amersham), and quantification of bands intensity using the Fuji image analysis software package.

Immunocytochemistry

The cultured cells were fixed with 4% paraformaldehyde (Wako, Osaka, Japan) and were permeabilized with 100% methanol. The cells were subsequently incubated overnight with relevant antibodies (dilution 1:50–100), and then incubated with FITC-labeled secondary antibody at dilution of 1:200 staining. The fluorescence was observed by a fluorescent microscope (Olympus, Tokyo, Japan). The nuclei were stained with DAPI, and the fluorescence was detected with a fluorescence microscope (Olympus). Image stacks were analyzed with the localization module of the Olympus software program (Olympus).

Uptake of Dil-Ac-LDL

The cells were incubated with cultured media containing 10 μg/ml acetylated low-density lipoprotein labeled 1,1′-dioctadecyl-3,3,3′,3′-tetramethyliodo-carbocyanine perchlorate (Dil-Ac-LDL; Biogenesis, Poole, England) at 37°C for 12 h. After incubation, the cells were photographed using a fluorescent microscope (Olympus).

Treatment of PnMECs with a conditioned medium of pericyte, angiopoietin-1, VEGF, or bFGF, and exposure of pericytes with TNF-α

The brain and peripheral nerve pericytes, astrocyte, and fibroblasts were cultured in DMEM with 20% FBS. After 24 h, the conditioned medium of brain pericytes (BPCT-CM), peripheral nerve pericytes (PPCT-CM) astrocytes (AST-CM), and fibroblasts (fibro-CM) was collected and stored at −20°C until analysis. The control medium was prepared by the same procedure using DMEM with 20% FBS (non-conditional medium (NCM)). PnMECs were treated with NCM, BPCT-CM, or PPCT-CM, or treated with angiopietin-1 (0, 0.1, 1, and 10 ng/ml), VEGF (0, 0.1, 1, and 10 ng/ml), or bFGF (0, 0.1, 1, and 10 ng/ml). Peripheral nerve pericytes were treated with DMEM with 10% FBS (NCM) and TNF-α (100 ng/ml). The total RNA was extracted 24 h later, and total protein was obtained after 3 days.

bFGF inhibitory study

PnMECs were cultured with PPCT-CM containing 1.0 μg/ml antibody against bFGF or normal rabbit IgG. The total RNA was extracted 24 h later, and total protein was obtained 3 days later.

Transendothelial electrical resistance (TEER) study

Transwell inserts (pore size 0.4 μm, effective growth area 0.3 cm^2, BD Bioscience, Franklin Lakes, NJ) were coated by rat-tail collagen type-I (BD Bioscience) according to the manufacturer's instructions. After PnMECs were seeded (1×10^6 cells/insert) in the upper compartment and cultured for 24 h, the upper compartment was incubated with each medium (NCM, EBM, BPCT-CM, and PPCT-CM) for 3 days. To construct in co-culture system, brain and peripheral nerve pericytes, astrocytes, or fibroblasts were seeded on the bottom side of the inserts. The cells were allowed to adhere firmly for overnight, and then endothelial cells were seeded on the upper side of the inserts placed in the well of the 24-well culture plates containing no cells, pericytes, or astrocytes. TEER values of cell layers were measured with a Millicell electrical resistance apparatus (Endohm-6 and EVOM; World Precision Instruments, Sarasota, FL). Statistical significance was evaluated using Student's *t*-test.

Transendothelial transport study

The paracellular passage of ^{14}C-labeled inulin (0.2 μCi/ml) across the cell layers was determined using previously described protocols. After 0.2 μCi of [carboxyl-^{14}C]-inulin in 0.5 ml of DMEM was added to the upper compartment, the appearance of [carboxyl-^{14}C]-inulin in the lower chamber was measured after 20 min by scintillation counting of 20 μl samples from the upper and lower chambers. The clearance (in μl) of inulin (C_{inu}) was calculated as $C_{inu} = V_L{}^{*}CPM_L/CPM_U$, where V_L is the volume of the lower compartment in μl, CPM_L is the radioactivity of [carboxyl-^{14}C]-inulin in the lower chamber in CPM/μl, and CPM_U is the radioactivity of [carboxyl-^{14}C]-inulin in the upper compartment in CPM/μl. The upper compartment was incubated with each medium (NCM, EBM, BPCT-CM, and PPCT-CM) for 3 days.

Data analysis

All data are presented as the mean ± SEM. The unpaired, two-tailed Student's *t*-test was used to determine the significance of differences between two group means. A *P*-value of <0.01 was considered to be statistically significant.

RESULTS

Characterization of human peripheral nerve and brain pericyte cell lines

Human peripheral nerve and brain pericyte cell lines were established (Fig. 1A–C). These two cell lines appeared to have a ruffled-border morphology with highly irregular edges, as shown in Figure 1A,B. The expression of the endothelial cell markers, *vWF* and *PECAM*, was not detected by RT-PCR in either cell line (Fig. 2A) and vWF expression was not detected by immunocytochemistry (Fig. 1D,E). These cell lines also did not take up Dil-Ac-LDL (Fig. 1G,H), thus indicating that they did not have the Ac-LDL receptor, which is an essential endothelial cell marker. We therefore confirmed that these cell lines were not contaminated by endothelial cells. We also isolated PnMECs of human BNB origin (Fig. 1C). Approximately 100% of the cells were immunoreactive for wWF (Fig. 1F) and they displayed the uptake of Dil-Ac-LDL (Fig. 1I).

The mRNA of several pericyte markers, such as *PDGF-Rβ*, *desmin*, and *osteopontin*, was detected by RT-PCR in the pericyte cell lines as well as in human brain tissue used as a positive control (Fig. 2A). The expression of αSMA and NG2 in these cell lines was verified by Western blot analysis (Fig. 2B,C) and immunocytochemistry (Fig. 2D,E) (Nehls and Drenckhahn, 1991; Ozerdem et al., 2001). They displayed stable growth and differentiated characteristics after at least five passages.

The peripheral nerve and brain pericytes cell lines expressed a large T-antigen with a molecular weight of 94 kDa under a permissive temperature of 33°C, which was the same molecular weight as that expressed by TR-BBB13 which expresses T-antigen at 33°C as a positive control (Hosoya et al., 2000) (Fig. 2F). Although hTERT protein was not detected by Western blot analysis (data not shown), these cell lines displayed a high expression level of nuclear and perinuclear hTERT protein by confocal microscopy (Fig. 2G,H). Therefore, pure BBB- and BNB-derived pericyte cell lines were successfully established from human tissue and identified the characteristics of the established pericyte cell lines.